

# Functional diversity in biters: the evolutionary morphology of the oral jaw system in pacus, piranhas and relatives (Teleostei: Serrasalminae)

ALESSIA HUBY<sup>1,\*</sup>, AURÉLIEN LOWIE<sup>1,3</sup>, ANTHONY HERREL<sup>2,3</sup>, RÉGIS VIGOUROUX<sup>4</sup>, BRUNO FRÉDÉRICH<sup>1</sup>, XAVIER RAICK<sup>1</sup>, GREGÓRIO KURCHEVSKI<sup>5</sup>, ALEXANDRE LIMA GODINHO<sup>5</sup> and ERIC PARMENTIER<sup>1</sup>

<sup>1</sup>Laboratory of Functional and Evolutionary Morphology, University of Liège, Liège, Belgium

<sup>2</sup>UMR7179 MNHN/CNRS, National Museum of Natural History, Paris, France

<sup>3</sup>Evolutionary Morphology of Vertebrates, Ghent University, Ghent, Belgium

<sup>4</sup>HYDRECO GUYANE, Laboratory Environment of Petit Saut, Kourou, French Guiana

<sup>5</sup>Fish Passage Center, Federal University of Minas Gerais, Belo Horizonte, Brazil

Received 14 December 2018; revised 14 March 2019; accepted for publication 14 March 2019

Serrasalminid fishes form a highly specialized group of biters that show a large trophic diversity, ranging from pacus able to crush seeds to piranhas capable of cutting flesh. Their oral jaw system has been hypothesized to be forceful, but variation in bite performance and morphology with respect to diet has not previously been investigated. We tested whether herbivorous species have higher bite forces, larger jaw muscles and more robust jaws than carnivorous species. We measured *in vivo* and theoretical bite forces in 27 serrasalminid species. We compared the size of the adductor mandibulae muscle, the jaw mechanical advantages, the type of jaw occlusion, and the size and shape of the lower jaw. We also examined the association between bite performance and functional morphological traits of the oral jaw system. Contrary to our predictions, carnivorous piranhas deliver stronger bites than their herbivorous counterparts. The size of the adductor mandibulae muscle varies with bite force and muscles are larger in carnivorous species. Our study highlights an underestimated level of functional morphological diversity in a fish group of exclusive biters. We provide evidence that the trophic specialization towards carnivory in piranhas results from changes in the configuration of the adductor mandibulae muscle and the lower jaw shape, which have major effects on bite performance and bite strategy.

**ADDITIONAL KEYWORDS:** adductor mandibulae muscle – bite force – diet – evolution – functional morphology – geometric morphometrics – lower jaw – trophic diversification.

## INTRODUCTION

Feeding performance is a determining factor for the survival and fitness of animals (Wainwright, 1988). In the animal kingdom, bite force (i.e. the ability of an animal to generate force with its jaws) is an important metric of whole-organism performance because of the relationship between jaw morphology and the feeding ecology of an animal (Anderson *et al.*, 2008). This trait of feeding performance has received increasing interest in recent decades and has been measured in a wide variety of vertebrate groups: sharks (e.g. Huber

*et al.*, 2005, 2006; Ferrara *et al.*, 2011; Rice *et al.*, 2016), teleosts (e.g. Hernandez & Motta, 1997; De Schepper *et al.*, 2008; Habegger *et al.*, 2017), amphibians (e.g. Deban & Richardson, 2017; Lappin *et al.*, 2017), lizards (e.g. Herrel *et al.*, 1999, 2001, 2004, 2014; Meyers *et al.*, 2018), turtles (e.g. Herrel *et al.*, 2002, 2017; Pfaller *et al.*, 2010), birds (e.g. van Der Meij & Bout, 2004; Herrel *et al.*, 2005; Rao *et al.*, 2018) and mammals (e.g. Aguirre *et al.*, 2002; Dumont & Herrel, 2003; Thomas *et al.*, 2015; Ginot *et al.*, 2018). Previous studies have demonstrated that bite force is usually related to body size (e.g. Erickson *et al.*, 2003; Huber *et al.*, 2006; Herrel *et al.*, 2014), cranial morphology (e.g. Herrel *et al.*, 2001; Lappin *et al.*, 2006; Da Silva *et al.*, 2016;

\*Corresponding author. E-mail: [alessia.huby@doct.uliege.be](mailto:alessia.huby@doct.uliege.be)

Dufour *et al.*, 2018), jaw muscle size (e.g. Raadsheer *et al.*, 1999; Herrel *et al.*, 2002; van der Meij & Bout, 2004) and mandible properties (e.g. Greaves, 2002; Nogueira *et al.*, 2009; Dollion *et al.*, 2017). Bite force usually varies with diet (e.g. Mehta, 2008; Nogueira *et al.*, 2009; Dollion *et al.*, 2017), prey type (e.g. Huber *et al.*, 2006; Santana *et al.*, 2010; Rao *et al.*, 2018) and food hardness (e.g. Aguirre *et al.*, 2003; van der Meij & Bout, 2006; Herrel & Holanova, 2008).

Ecomorphological studies devoted to studying variations in the feeding apparatus (i.e. oral and pharyngeal jaws, head and digestive tract morphology) in teleost fishes are plentiful. Cichlids are probably the best studied fish taxa regarding their diversity of trophic morphology (Liem, 1993; Albertson & Kocher, 2006; Cooper *et al.*, 2011) but several other families such as Labridae (Wainwright *et al.*, 2004), Apogonidae (Barnett *et al.*, 2006), Pomacanthidae (Konow & Bellwood, 2005, 2011), Cyprinidae (Hernandez & Staab, 2015), Chaetodontidae (Konow *et al.*, 2017) and Pomacentridae (Frédérich *et al.*, 2008a, b) have also been explored. Compared with other vertebrates, teleosts vary largely in their feeding modes with three generally recognized methods of prey capture (Liem, 1993): suction-feeding, ram-feeding and biting. Most studies have illustrated functional morphological variation associated with diet specialization in fish taxa including various feeding modes. For example, the disparate trophic groups of wrasses (e.g. Wainwright *et al.*, 2004) and cichlids (e.g. Cooper *et al.*, 2011) include biters, suction-feeders and ram-feeders and a large amount of functional morphological disparity is explained by evolutionary shifts between feeding modes. Surprisingly, few studies (but see Konow & Bellwood, 2011) have explored the functional morphological variation in fish clades showing a large diversity of diet despite being based on a single feeding mode.

Serrasalminae, a monophyletic family of South American freshwater fishes, is atypical among Neotropical characiforms because of its trophic diversification (Correa *et al.*, 2007) and its exclusively 'biting' feeding mode on diverse prey items (e.g. fishes, other vertebrates, fins, scales, crustaceans, molluscs, insects, aquatic plants, flowers, fruits, seeds, algae). According to recent molecular phylogenies, Serrasalminae (~98 species) is divided into three major subclades (Supporting Information, Fig. S1): (1) the 'pacus-clade' including the herbivorous genera *Colossoma*, *Mylossoma* and *Piaractus*; (2) the 'myleus-clade' with the herbivorous genera *Mylesinus*, *Myleus*, *Myloplus*, *Ossubtus*, *Tometes* and *Utiaritchthys*; and (3) the 'piranhas-clade' with the lepidophagous genus *Catoprion*, the herbivorous genus *Metynniss* and the carnivorous genera *Pristobrycon*, *Pygocentrus*, *Pygopristis* and *Serrasalmus* (Thompson *et al.*, 2014).

The herbivorous genus *Acnodon* may be considered as the sister-group of the 'myleus-clade' (Ortí *et al.*, 1996, 2008; Calcagnotto *et al.*, 2005; Thompson *et al.*, 2014). Interestingly, serrasalmin species diversified into various feeding habits that are all dependent on biting and oral manipulation, suggesting the ability to generate bite force as a basal trait. The different trophic guilds of serrasalmins range from the pacus, capable of crushing hard-shelled fruits and seeds, to the piranhas capable of slicing pieces of fleshy prey (Correa *et al.*, 2007) but also include the wimple piranha, *Catoprion mento*, which specializes on extracting scales (Janovetz, 2005). This fish family offers us the opportunity to test in a phylogenetic context (1) how bite performance varies within a group of highly specialized biters and (2) which morphological and functional traits of the oral jaw system vary in accordance with bite performance and diet specialization.

The black piranha, *Serrasalmus rhombeus*, may hold the record for relative bite force among extant vertebrate taxa (Grubich *et al.*, 2012). The force of its jaws is, proportionally to body size, up to three times stronger than the bite force for a great white shark (Wroe *et al.*, 2008; Ferrara *et al.*, 2011) or an adult alligator (Erickson *et al.*, 2003). In addition to an extreme jaw force, the black piranha has a single row of highly specialized sharp and triangular teeth on each jaw allowing it to cut small pieces of flesh from larger animals (Shellis & Berkovitz, 1976; Jégu, 2003). In contrast, the herbivorous pacus, *Colossoma macropomum* and *Piaractus brachipomus*, have one or two rows of specialized multicuspid incisiform-to-molariform teeth on the lower and upper jaws respectively, which are adapted for crushing fruits and hard-shelled seeds (Goulding, 1980; Goulding & Carvalho, 1982; Jégu, 2003). Differences in digestive tract length have also been highlighted between carnivorous and herbivorous serrasalmins (Pelster *et al.*, 2015). Other possible morphological and performance changes in jaws and associated muscles have, however, never been investigated and compared between dietary groups. So, how do bite performance and buccal morphological traits vary between carnivorous piranhas and their herbivorous counterparts?

In this study, we aim to conduct a comparative functional morphological analysis of the oral jaw system in the Neotropical family Serrasalminae. We hypothesize that herbivorous species that mainly feed by crushing hard plant items (fruits and seeds) should have higher bite forces than carnivorous species that feed on soft animal prey (meat and flesh). In addition, species with a more durophagous diet should have more strongly developed muscles and more robust jaws than carnivorous species. We here seek to (1) determine bite forces empirically and theoretically

in serrasalmid species with varied feeding habits (carnivorous and herbivorous), (2) investigate the association between bite performance and diet, (3) compare the morphology and functional properties of the oral jaw system between dietary groups and (4) explore whether the studied functional morphological traits may explain bite performance in serrasalmids.

## MATERIAL AND METHODS

### FISH SAMPLING AND DIET INFORMATION

We studied a total of 647 specimens from 27 serrasalmid species (Table 1). Additional information about sampling, provenance and maintenance of serrasalmid species are given in the Supporting Information (Text S1). We used live specimens from 20 species from nine different genera to record *in vivo* bite forces ( $BF_{in\ vivo}$ ). Specimens from 22 species, including seven additional species and two other genera, were euthanized to estimate theoretical bite forces ( $BF_{theoretical}$ ) from the adductor mandibulae muscle (which closes the lower jaw and is therefore responsible for the bite). Specimens used for this last approach were euthanized by an overdose of ethyl 3-aminobenzoate methanesulfonate 98% (MS-222, Sigma Aldrich) dissolved in water. Several of these specimens also came from two other studies in our laboratory (Mélotte *et al.*, 2016, 2018). Specimens from 15 species studied via the above two methods were used to assess the validity of our bite force estimates. In addition, euthanized specimens were used for dissections, calculations of jaw mechanical advantages and type of jaw occlusion, and landmark-based geometric morphometric analyses.

In serrasalmid fishes, tooth shape and dentition patterns can be used as a reliable proxy of diet (e.g. Géry, 1972; Goulding, 1980; Nico & Taphorn, 1988; Jégu, 2003; Supporting Information, Table S1). We thus grouped species into two main dietary categories based on their dentition (Fig. S2): carnivorous and herbivorous species (Table 1). *Catoprion mento*, a specialist lepidophagous species, formed a third category but we did not include it in comparative statistical analyses.

### BITE FORCES

#### *In vivo* bite forces

We recorded *in vivo* bite forces in 543 live specimens of 20 serrasalmid species (Table 1) using a piezo-electric and isometric Kistler force transducer (type 9203, range  $\pm 500$  N, Kistler Inc.; see Herrel *et al.*, 1999). For each bite session, we caught fish in their aquarium or in their natural environment using fishing nets or hook-and-lines. Fishes were then held by hand and we

measured *in vivo* bite forces by introducing bite plates between the oral jaws. For each specimen, we recorded three to five consecutive ‘aggressive’ or ‘crushing’ bites depending on diet. The point of application of the bite force was standardized by the fixed length of the bite plates. We retained the highest recorded bite force value as the maximal  $BF_{in\ vivo}$  value for the animal (Herrel *et al.*, 1999) although this value may in some cases reflect a maximum effort and not a physiological limit for the specimen (Astley *et al.*, 2013). We corrected these maximal  $BF_{in\ vivo}$  values by the lever arms of the set-up (i.e. the distance from the bite point to the fulcrum) before using them in further analyses.

For each specimen, we also directly measured the standard length (SL) using a calliper or photographs where the specimen was positioned on graph paper for scale. We obtained body mass (BM) using a normal balance (max = 3 kg; Silvercrest) or a spring scale (max = 100, 2500, 5000 or 10 000 g; PESOLA).

All procedures and methods applied in this study were approved by the Animal Care and Use Committee of the University of Liège, Belgium (ethics case 1835). All experiments were performed in accordance with the Guide for the Care and Use of Laboratory Animals.

#### Theoretical bite forces

We isolated the right adductor mandibulae muscle and lower jaw in 158 euthanized specimens of 22 serrasalmid species (Table 1) under a binocular microscope (Leica Wild M10). From the adductor mandibulae muscle, we estimated  $BF_{theoretical}$  using standard equations of (1) muscle physiological cross-sectional area (PCSA, Powell *et al.*, 1984), (2) maximum isometric muscle force ( $F_{max}$ , e.g. Huber *et al.*, 2006) and (3) output force ( $F_{out}$ , e.g. Moran & Ferry, 2014) for each muscle subdivision of the adductor mandibulae muscle (Supporting Information, Text S2). For each specimen, we added up the output forces of each muscle subdivision and then duplicated the total jaw force to account for the bilateral bite to determine a value for  $BF_{theoretical}$ .

### FUNCTIONAL MORPHOLOGICAL TRAITS OF THE ORAL JAW SYSTEM

#### Adductor mandibulae muscle

In the same 158 specimens (Table 1), we recorded the origin sites of the adductor mandibulae muscle on the skull and suspensorium. We then completely removed the right ‘adductor-mandibulae-lower-jaw’ complex and recorded the insertion sites of the different muscle subdivisions. We also photographed the muscle subdivisions using a camera (Canon EOS 6D digital, Canon Inc.) with graph paper in view for scale. The

**Table 1.** Summary of diet, fish sampling, body size, and *in vivo* and theoretical bite forces in 27 serrasalmid species included in this comparative study

Diet	Genus	Species name	Live specimens			Euthanized specimens					
			<i>N</i>	BM (g)	SL (mm)	BF <sub><i>in vivo</i></sub> (N)	<i>N</i>	BM (g)	SL (mm)	BF <sub>theoretical</sub> (N)	
			total								
Carnivorous	<i>Pristobrycon</i>	<i>Pristobrycon striolatus</i>	7								
	<i>Pygocentrus</i>	<i>Pygocentrus cariba</i>	2								
		<i>Pygocentrus nattereri</i>	218	294 ± 339	182 ± 55	84 ± 68	23	79 ± 161	103 ± 42	20 ± 22	
	<i>Pygopristis</i>	<i>Pygocentrus piraya</i>	17	1886 ± 2033	269 ± 144	75 ± 63	8	49 ± 26	104 ± 15	22 ± 9	
		<i>Pygopristis denticulata</i>	14	49 ± 28	106 ± 25	15 ± 7	10	25 ± 30	77 ± 33	5 ± 5	
	<i>Serrasalmus</i>	<i>Serrasalmus brandtii</i>	35	230 ± 140	186 ± 42	30 ± 17					
		<i>Serrasalmus compressus</i>	5				5	6 ± 2	73 ± 5	3 ± 1	
		<i>Serrasalmus elongatus</i>	10	23 ± 3	109 ± 7	8 ± 1	8	8 ± 9	79 ± 23	3 ± 3	
	Herbivorous	<i>Serrasalmus</i>	<i>Serrasalmus humeralis</i>	5				5	27 ± 7	102 ± 9	12 ± 3
			<i>Serrasalmus maculatus</i>	40	361 ± 183	209 ± 44	61 ± 26				
		<i>Serrasalmus</i>	<i>Serrasalmus manueli</i>	4	56 ± 9	124 ± 6	24 ± 2	3	59 ± 5	127 ± 4	25 ± 15
			<i>Serrasalmus marginatus</i>	61	120 ± 41	169 ± 17	28 ± 13	6	3 ± 1	60 ± 3	1 ± 1
		<i>Serrasalmus</i>	<i>Serrasalmus rhombeus</i>	3				3	39 ± 1	108 ± 8	15 ± 3
			<i>Serrasalmus spilopleura</i>	7	19 ± 15	84 ± 12	10 ± 5	4	21 ± 12	85 ± 10	10 ± 6
			<i>Acnodon oligacanthus</i>	3				3	37 ± 6	115 ± 7	4 ± 1
<i>Colossoma</i>	<i>Colossoma</i>	<i>Colossoma macropomum</i>	5	70 ± 72	120 ± 50	15 ± 9	3	21 ± 14	86 ± 21	4 ± 2	
		<i>Metynnus hypsauchen</i>	11	9 ± 13	55 ± 28	2 ± 2	2	12 ± 11	62 ± 20	2 ± 1	
	<i>Metynnus</i>	<i>Metynnus lippincottianus</i>	9	39 ± 4	103 ± 3	4 ± 1	6	37 ± 17	90 ± 15	3 ± 2	
		<i>Metynnus maculatus</i>	78	104 ± 34	136 ± 15	3 ± 1					
	<i>Myleus</i>	<i>Myleus micans</i>	4	2525 ± 613	405 ± 40	14 ± 3					
<i>Myloplus</i>	<i>Myloplus</i>	<i>Myloplus rhomboidealis</i>	2				2	32 ± 1	94 ± 1	11 ± 1	
		<i>Myloplus rubripinnis</i>	12	50 ± 19	120 ± 27	5 ± 6	4	30 ± 13	87 ± 14	3 ± 1	
	<i>Myloplus</i>	<i>Myloplus schomburgkii</i>	18	22 ± 6	82 ± 8	9 ± 4	12	25 ± 6	85 ± 9	5 ± 1	
		<i>Myloplus ternetzi</i>	24	129 ± 100	138 ± 37	5 ± 4	22	87 ± 70	121 ± 31	7 ± 4	
<i>Piaractus</i>	<i>Piaractus</i>	<i>Piaractus brachypomus</i>	34	574 ± 1165	164 ± 131	26 ± 38	15	60 ± 63	112 ± 43	9 ± 8	
		<i>Piaractus mesopotamicus</i>	13	3581 ± 605	502 ± 25	93 ± 13					
	<i>Catoprion</i>	<i>Catoprion mento</i>	6	35	103	2	5	5 ± 4	58 ± 10	1 ± 1	

Additional information and references regarding serrasalmid diet are given in Table S1. In some cases, the total fish sampling is not consistent with the sum of sample sizes for *in vivo* and theoretical bite forces because the sample size of theoretical bite forces includes euthanized specimens from live specimens of the present study as well as preserved specimens from other studies (Mélotte *et al.*, 2016, 2018). Body size and bite force entries are means ± SD. The lepidophagous species *Catoprion mento* was not included in comparative statistical analyses. Abbreviations: BF<sub>*in vivo*</sub>, *in vivo* bite force; BF<sub>theoretical</sub>, theoretical bite force; BM, body mass; *N*, sample size; *N* total, total fish sampling; SL, standard length.

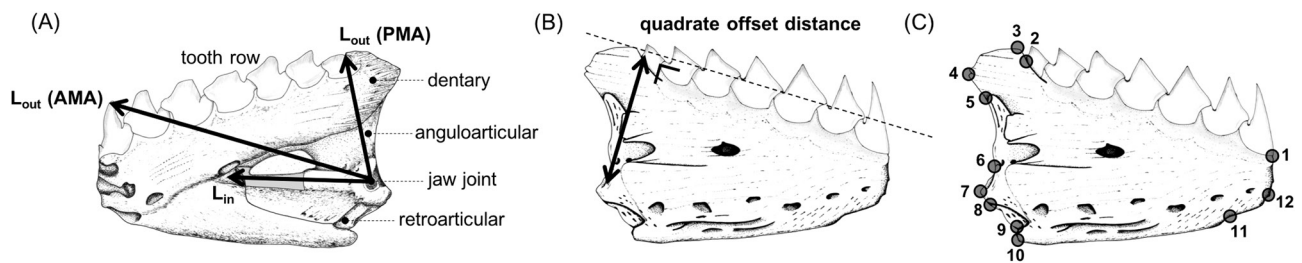


**Figure 1.** Schematic representations in medial (A) and lateral view (B, C) of the lower jaw of the carnivorous *Pygocentrus nattereri* and illustrations of the measurements of: A, anterior and posterior mechanical advantages, AMA and PMA respectively, with the in-lever arm,  $L_{in}$ , and the out-lever arm,  $L_{out}$ ; B, quadrature offset distance; and C, landmarks for the geometric morphometric analysis. The identification of landmark numbers is: (1) the most anterior point of the dentary at the level of the tooth row; (2) the posterior point of the dentary behind the tooth row; (3) the most dorsal point of the coronoid process of the dentary; (4) the most posterior point of the coronoid process of the dentary; (5) the most posterior point between the coronoid process of the dentary and the anguloarticular; (6) the most posterodorsal point of the anguloarticular above the jaw joint; (7) the most posteroventral point of the anguloarticular beneath the jaw joint; (8) the most posterodorsal point of the retroarticular; (9) the most posteroventral point of the retroarticular; (10) the most posteroventral point of the dentary; (11) the most ventral point of the dentary symphysis; and (12) the most anteroventral point of the dentary symphysis.

terminology of [Datovo & Vari \(2013\)](#) was used to describe the subdivisions of the adductor mandibulae muscle. For each muscle subdivision, we obtained muscle mass using a Cobos precision balance ( $\pm 0.001$  g, type M-150-SX). In addition, for each specimen, we calculated the percentage of the adductor mandibulae muscle relative to body mass and the percentage of each muscle subdivision relative to the total adductor mandibulae muscle mass.

#### *Jaw mechanical advantages*

The force transmission of the adductor mandibulae muscle to the lower jaw can be determined by the mechanical advantage, which is the ratio of the in-lever arm ( $L_{in}$ , distance between the jaw joint and the muscle insertion onto the lower jaw) and the out-lever arm ( $L_{out}$ , distance between the jaw joint and the application point of bite force) ([Westneat, 2004](#)) ([Fig. 1A](#)). For each muscle subdivision, we calculated anterior and posterior mechanical advantages (AMA and PMA, respectively) according to [Anderson \(2009\)](#) to examine whether muscle subdivisions have a different force transmission. We measured the out-lever arm for AMA from the jaw joint to the anterior tip of the lower jaw. We then measured the out-lever arm for PMA from the jaw joint to the most posterior tip of the tooth row on the lower jaw. Lever arm ratios are dimensionless.

#### *Type of jaw occlusion*

To determine whether bite strategy differs between carnivorous and herbivorous serrasalmid species, we measured the quadrature offset distance of the lower jaw following the method of [Anderson \(2009\)](#). The

quadrature offset distance is a metric that can be used to estimate the type of jaw occlusion. This metric represents the orthogonal distance between the quadrature–anguloarticular joint of the lower jaw and the dentition. The shorter the distance, the more imperfect is the occlusion between upper and lower jaws as in a ‘scissor-like’ system. The higher the distance, the more perfect is the jaw occlusion as in a ‘vice-like’ system. For each specimen, we photographed the right lower jaw in lateral view using a camera (Canon EOS 6D digital) with the jaw positioned on graph paper for scale. We then drew a line tangential to the tooth row passing by the jaw joint on each photograph. We measured the direct distance between this line and the jaw joint as the quadrature offset distance ([Fig. 1B](#)). Finally, we divided this value by the overall length of the lower jaw to make the value dimensionless.

#### *Size and shape of the lower jaw*

We used 12 homologous landmarks to capture shape variation of the lower jaw ([Fig. 1C](#)). We digitized the x- and y-coordinates of each landmark from photographs of the lateral view of the right lower jaw using the morphometric software TPSDig v.1.40 (F. J. Rohlf, 2004, <http://life.bio.sunysb.edu/morph/>; accessed 30 March 2019). We then conducted a Generalized Procrustes Analysis (GPA) to align specimens to a common coordinate system and remove variation in their position, orientation and size ([Rohlf & Slice, 1990](#)). Next, we determined the lower jaw size for each specimen from the landmark configurations as centroid size, i.e. the square root of summed squared distances of landmarks from the centroid ([Bookstein,](#)

1991). The Procrustes tangent coordinates were used as shape variables for all specimens (Adams *et al.*, 2013). Finally, we calculated mean configurations for each species from size and shape variables.

#### STATISTICAL ANALYSES

Bite force, body mass and jaw muscle mass data were  $\log_{10}$ -transformed before statistical analyses to meet assumptions of normality and homoscedasticity. Jaw mechanical advantages, quadrate offset distance and lower jaw shape data were not transformed because they are dimensionless. For each variable, we calculated a mean value per species. To take into account the variation in body mass in serrasalmid fishes (Azevedo, 2010), we regressed the  $\log_{10}$ -transformed  $BF_{in\ vivo}$ ,  $BF_{theoretical}$  and adductor mandibulae muscle mass against the  $\log_{10}$ -transformed body mass (Habegger *et al.*, 2017). In addition, we regressed the  $\log_{10}$ -transformed muscle mass of each jaw muscle subdivision against the  $\log_{10}$ -transformed adductor mandibulae muscle mass. Residuals from these regressions were used in statistical analyses.

First, we tested for divergence in relative bite performance ( $BF_{in\ vivo}$  and  $BF_{theoretical}$ ) between carnivorous and herbivorous species. A divergence in bite performance between dietary groups may result from a difference in slope and/or intercept of the bite force vs. body mass relationship (van der Meij & Bout, 2004). We performed an analysis of covariance (ANCOVA) with diet as factor and body mass as covariate to test for the homogeneity of slopes and intercept divergence for the two groups. We also determined whether  $BF_{theoretical}$  is a good predictor of  $BF_{in\ vivo}$  using a linear regression of  $BF_{in\ vivo}$  and  $BF_{theoretical}$  mean values (Santana *et al.*, 2010).

Next, we tested for morphological variation of the adductor mandibulae muscle and its muscle subdivisions between carnivorous and herbivorous species. We compared slopes and intercepts of the linear regressions on  $\log_{10}$ -transformed jaw muscle mass data using ANCOVAs (van der Meij & Bout, 2004). We also determined for each species the mean percentage of the adductor mandibulae muscle relative to body mass as well as the mean percentage of the mass of each muscle subdivision relative to the total adductor mandibulae muscle mass. We then tested for differences in these mean percentages between dietary groups using the non-parametric Mann–Whitney *U* test. Similarly, we evaluated the functional variation of the oral jaw system between carnivorous and herbivorous species using non-parametric Mann–Whitney *U* tests on jaw mechanical advantages and quadrate offset distance.

To compare independently the size and shape of the lower jaw between dietary groups, we tested for

differences in lower jaw size (i.e. centroid size) and shape between carnivorous and herbivorous species using a Procrustes ANOVA with diet as factor (Collyer *et al.*, 2015). We also carried out a principal components analysis (PCA) on shape variables to explore lower jaw shape variation among species and dietary groups. Deformation grids were used to describe the trends of the lower jaw shape variation along PC axes.

Next, we tested for the hypothetical association between the size of the adductor mandibulae muscle and bite force ( $BF_{in\ vivo}$ ) using a linear regression. Similarly, we explored hypothetical relationships between  $BF_{in\ vivo}$  and the other functional morphological traits of the oral jaw system, i.e. jaw mechanical advantages (AMAs and PMAs), type of jaw occlusion (quadrate offset distance) and lower jaw shape (PC1 axis, which explains 85% of the total shape variation – see Results). Finally, to identify which functional morphological traits best explain the variability in  $BF_{in\ vivo}$ , we conducted a stepwise multiple linear regression with  $BF_{in\ vivo}$  as the response variable and adductor mandibulae muscle mass, mean AMA, mean PMA, quadrate offset distance and PC1 as predictor variables and we kept the final model (Herrel *et al.*, 2014).

As a first step, we conducted regular statistical analyses but we also used phylogenetically corrected statistical methods (Revell, 2009) such as phylogenetic generalized least squares (PGLS) regressions and phylomorphospace analyses because species are not phylogenetically independent (Felsenstein, 1985). The regular statistics allowed the study of all species, while the phylogenetically corrected analyses excluded nine species from our study (*Metynnis lippincottianus*, *Metynnis maculatus*, *Myleus micans*, *Myloplus ternetzi*, *Piaractus mesopotamicus*, *Pygocentrus cariba*, *Serrasalmus brandtii*, *Serrasalmus elongatus* and *Serrasalmus maculatus*) because no phylogenetic information is available for these species. For this reason, we first described results from statistics without phylogenetic correction.

All statistical analyses were conducted in the R environment (R Core Team, 2017), except slope homogeneity tests which were implemented in PAST 3.13 (Hammer *et al.*, 2001). All analyses of shape variation were performed using the R package ‘geomorph’ (Adams & Otárola-Castillo, 2013; Adams *et al.*, 2017) and phylogenetic comparative analyses using the R packages ‘geiger’ (Harmon *et al.*, 2007) and ‘phytools’ (Revell, 2012).

## RESULTS

### BITE FORCES

Absolute mean values of  $BF_{in\ vivo}$  (Table 1) range widely between the herbivorous *Piaractus mesopotamicus* with the highest value ( $93 \pm 13$  N,

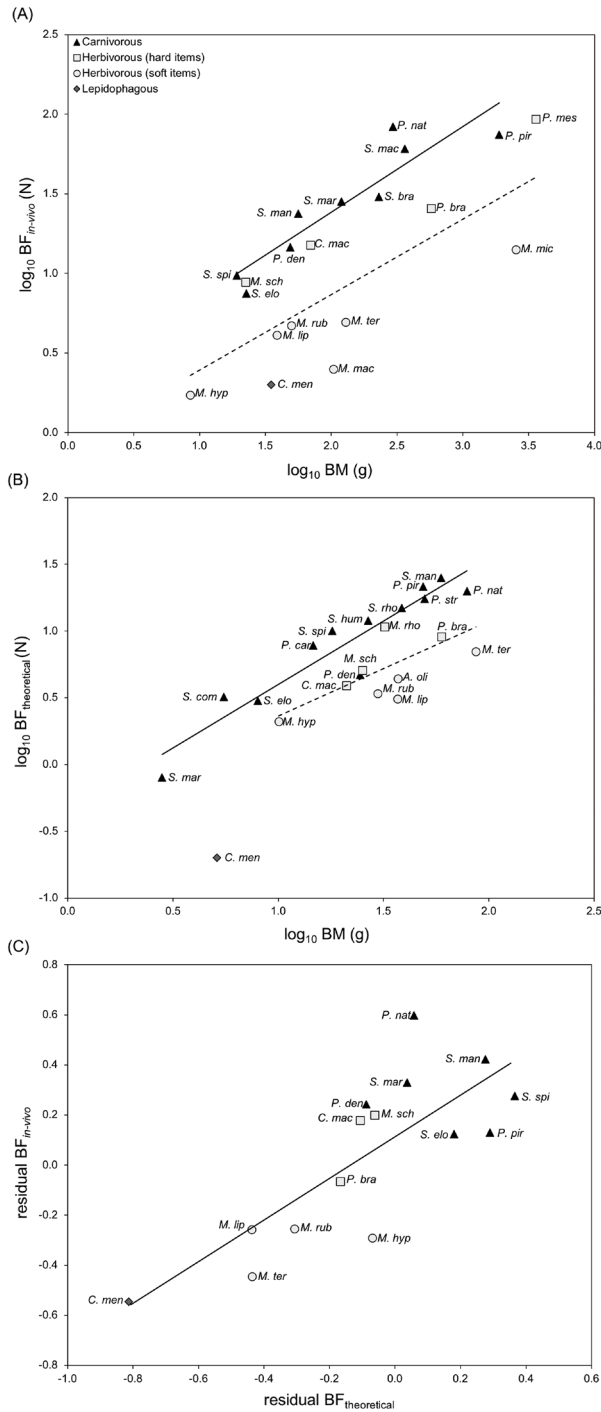


**Figure 2.** Linear regressions of: (A)  $\log_{10}$ -transformed *in vivo* bite force ( $\log_{10} \text{BF}_{in vivo}$ ) against  $\log_{10}$ -transformed body mass ( $\log_{10} \text{BM}$ ) in 20 species; (B)  $\log_{10}$ -transformed theoretical bite force ( $\log_{10} \text{BF}_{theoretical}$ ) against  $\log_{10}$ -transformed body mass ( $\log_{10} \text{BM}$ ) in 22 species; and (C) residual *in vivo* bite force ( $\text{BF}_{in vivo}$ ) and residual theoretical bite force ( $\text{BF}_{theoretical}$ ) in 15 serrasalmid species with different diet. Key in A applies also to B and C. *Catoprion mento* was not included in comparative statistical analyses.

mean  $\pm$  SD), the carnivorous *Pygocentrus nattereri* ( $84 \pm 68$  N), the herbivorous *Myloplus schomburgkii* ( $9 \pm 4$  N) and the lepidophagous *Catoprion mento* with the lowest value (2 N). Body size (i.e. body mass) positively and significantly influences *in vivo* bite force in serrasalmid fishes (all species:  $r = 0.70$ ; carnivorous:  $r = 0.91$ ; herbivorous:  $r = 0.79$ ; all  $P < 0.01$ ). Slopes of this linear model do not vary between carnivorous and herbivorous species (slope homogeneity test:  $F = 0.13$ ,  $P = 0.73$ ) but the intercepts vary significantly (ANCOVA:  $F_{1,16} = 17.61$ ,  $P < 0.001$ ,  $\eta^2_p = 0.69$ ). Carnivorous species show higher relative  $\text{BF}_{in vivo}$  than herbivorous species (Fig. 2A). Phylogenetic ANCOVA is, however, not significant (Table 2), indicating that diet does not explain divergence in  $\text{BF}_{in vivo}$  considering the phylogenetic configuration used in this study (Supporting Information, Fig. S1). Additionally, note that the *in vivo* bite force data presented here can be influenced by several factors such as sample size, animal motivation, age, captive state and physiological conditions of the bite.

Similarly, slopes of the linear model of  $\text{BF}_{theoretical}$  against body mass do not vary between carnivorous and herbivorous species (slope homogeneity test:  $F = 2.25$ ,  $P = 0.15$ ) but the intercepts vary significantly (ANCOVA:  $F_{1,18} = 9.79$ ,  $P < 0.05$ ,  $\eta^2_p = 0.80$ ). Carnivorous species show higher relative  $\text{BF}_{theoretical}$  than herbivorous species (Fig. 2B) but this variation is not supported by phylogenetic ANCOVA (Table 2). Moreover,  $\text{BF}_{theoretical}$  from the adductor mandibulae muscle is a reasonably good predictor of  $\text{BF}_{in vivo}$  in the 15 serrasalmid species for which we have both estimates ( $R^2 = 0.63$ ,  $P < 0.001$ ; Fig. 2C). This linear model can thus be used to approximate bite performance of serrasalmid species for which  $\text{BF}_{in vivo}$  is not available.

#### ANATOMICAL DESCRIPTION OF THE ADDUCTOR MANDIBULAE MUSCLE

The adductor mandibulae muscle is divided into a segmentum facialis and a segmentum mandibularis. Both muscle segments are connected via a strong

In A, regression line equations are  $\log_{10} \text{BF}_{in vivo} = 0.54 \log_{10} \text{BM} + 0.31$  ( $R^2 = 0.84$ ) for carnivorous species and  $\log_{10} \text{BF}_{in vivo} = 0.47 \log_{10} \text{BM} - 0.08$  ( $R^2 = 0.62$ ) for herbivorous species. In B, these equations are  $\log_{10} \text{BF}_{theoretical} = 0.95 \log_{10} \text{BM} - 0.35$  ( $R^2 = 0.90$ ) for carnivorous species and  $\log_{10} \text{BF}_{theoretical} = 0.58 \log_{10} \text{BM} - 0.20$  ( $R^2 = 0.45$ ) for herbivorous species. In C, each point represents the species residual mean of two bite force measurements, and the equation of the regression line is  $\text{residual BF}_{in vivo} = 0.84 \text{residual BF}_{theoretical} + 0.12$  ( $R^2 = 0.63$ ). Abbreviations of species names are given in Table S1.

tendinous complex termed the intersegmental aponeurosis. The segment of the cheek, the segmentum facialis, is subdivided into three subdivisions (Fig. 3).

- The pars rictalis attaches onto the lower jaw on the coronoid process of the dentary and on the anguloarticular bone (Fig. 3C, D). This subdivision may have different sites of origin on the suspensorium depending on diet: (1) the horizontal and vertical arms of the preoperculum as well as the quadrate bone in all herbivorous species and (2) only the horizontal arm of the preoperculum and the quadrate bone in the lepidophagous *Catoprion mento* and most carnivorous species (Fig. 3A, B). However, we recorded that the pars rictalis of the carnivorous *Pygopristis denticulata* and *Pristobrycon striolatus* also originates on the vertical arm of the preoperculum (Table S2).
- The *pars malaris* is strongly attached to the lower jaw mainly via the intersegmental aponeurosis tendinous complex that divides into a Meckelian tendon inserting onto the coronomeckelian bone and a mandibular tendon inserting onto the dentary (Fig. 3C, D). The main sites of origin of the *pars malaris* are on the skull and suspensorium (i.e. the neurocranium, the hyomandibula, the vertical arm of the preoperculum, the metapterygoid and the quadrate–metapterygoid window). However, variations may also be present depending on diet: the muscle fibres (1) only attach on the lateral surface of the hyomandibula in herbivorous species such as *Metynnis hypsauchen*, *Metynnis lippincottianus* and *Myloplus ternetzi*, (2) attach onto the lateral surface of the hyomandibula and on a small portion of the hyomandibula–neurocranium joint in other herbivorous species and the lepidophagous *Catoprion mento*, and (3) attach both onto the lateral and medial surfaces of the hyomandibula and on a large portion of the hyomandibula–neurocranium joint in carnivorous species (Table S2).
- The pars stegalis attaches onto the lower jaw via a short tendon joining the intersegmental aponeurosis tendinous complex at the level of the mandibular tendon (Fig. 3C, D). This subdivision may have divergent sites of origin depending on diet: the muscle fibres (1) only attach on the metapterygoid in all herbivorous species and the lepidophagous *Catoprion mento* and (2) attach on the metapterygoid and the sphenoid bone of the neurocranium in all carnivorous species, except for *Pygopristis denticulata* in which it more closely resembles that in herbivorous species (Table S2).

**Table 2.** Results of phylogenetic comparative methods used in this study

Formula	df	Intercept ± SE	Slope ± SE	t	P
<b>Phylogenetic regressions (PGLS)</b>					
log <sub>10</sub> adductor mandibulae muscle mass ~ log <sub>10</sub> BM	17	-2.39 ± 0.19	1.1 ± 0.07	15.61	<0.001
log <sub>10</sub> pars rictalis ~ log <sub>10</sub> adductor mandibulae muscle mass	17	-0.34 ± 0.12	1.18 ± 0.05	24.93	<0.001
log <sub>10</sub> <i>pars malaris</i> ~ log <sub>10</sub> adductor mandibulae muscle mass	17	-0.27 ± 0.04	0.98 ± 0.02	61.61	<0.001
log <sub>10</sub> pars stegalis ~ log <sub>10</sub> adductor mandibulae muscle mass	17	-1.06 ± 0.14	1.12 ± 0.05	21.27	<0.001
phylo residuals BF <sub>in vivo</sub> ~ phylo residuals adductor mandibulae muscle mass	11	0 ± 0.2	0.7 ± 0.46	0.14	0.89
<b>Phylogenetic ANCOVAs</b>					
log <sub>10</sub> BF <sub>in vivo</sub> ~ diet + log <sub>10</sub> BM	9	1.53	0.17	5.26	0.3
log <sub>10</sub> BF <sub>theoretical</sub> ~ diet + log <sub>10</sub> BM	15	2.36	0.16	2	0.58
log <sub>10</sub> adductor mandibulae muscle mass ~ diet + log <sub>10</sub> BM	15	2.75	0.18	4.48	<b>0.05</b>
log <sub>10</sub> pars rictalis mass ~ diet + log <sub>10</sub> adductor mandibulae muscle mass	15	3.9	0.26	0.44	0.52
log <sub>10</sub> <i>pars malaris</i> mass ~ diet + log <sub>10</sub> adductor mandibulae muscle mass	15	2.63	0.18	10.33	< <b>0.05</b>
log <sub>10</sub> pars stegalis mass ~ diet + log <sub>10</sub> adductor mandibulae muscle mass	15	3.77	0.25	3.44	0.08

The table first presents the main results of the phylogenetic regressions (PGLS) and then phylogenetic ANCOVAs. Abbreviations: BF<sub>in vivo</sub>, *in vivo* bite force; BF<sub>theoretical</sub>, theoretical bite force; BM, body mass; df, degrees of freedom; F, value of the F-statistic; P, probability of significant difference between groups; SE, standard deviation; t, value of the t-statistic. Significant values are given in bold type.

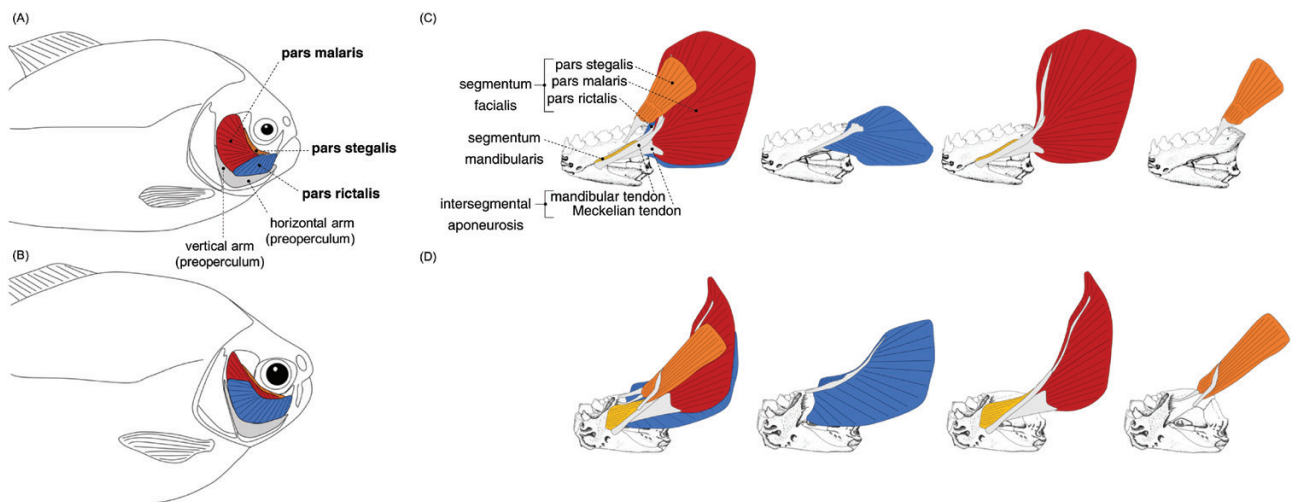


**Figure 3.** Schematic illustrations in lateral (A, B) and medial (C, D) view of the adductor mandibulae muscle and its three main subdivisions attached to the right lower jaw in the carnivorous *Pygocentrus nattereri* (A, C) and the herbivorous *Piaractus brachyomus* (B, D). The adductor mandibulae muscle is divided into the segmentum mandibularis represented in yellow and the segmentum facialis subdivided into three muscle subdivisions: the pars rictalis in blue, the *pars malaris* in red and the *pars stegalis* in orange. A and B, the preoperculum bone is represented in grey with its vertical and horizontal arms. C and D, the intersegmental aponeurosis tendinous complex is represented in light grey and is primarily subdivided into mandibular tendon and Meckelian tendon. Drawings are made to scale.

#### SIZE OF THE ADDUCTOR MANDIBULAE MUSCLE AND ITS SUBDIVISIONS

The adductor mandibulae muscle is four times heavier with respect to body mass in carnivorous ( $1.6 \pm 0.4\%$ , mean  $\pm$  SD) than in herbivorous species ( $0.4 \pm 0.2\%$ ; Figs 4A, S3A; Table 3). The jaw muscle of the lepidophagous *Catoprion mento* is even smaller ( $0.2 \pm 0.1\%$ ). In addition, the mass of the three main muscle subdivisions of the adductor mandibulae muscle differ between dietary groups. The pars rictalis is four times larger in herbivorous ( $43.1 \pm 4.2\%$ ) than in carnivorous species ( $10.5 \pm 4.9\%$ ; Figs 4B, S3B; Table 3). The *pars malaris* is almost twice as large in carnivorous ( $83 \pm 5.9\%$ ) than in herbivorous species ( $50.6 \pm 5.9\%$ ; Figs 4C, S3C; Table 3). The *pars stegalis* is equivalent in carnivorous ( $6.5 \pm 2.1\%$ ) and herbivorous species ( $6.2 \pm 0.3\%$ ; Figs 4D, S3D; Table 3). Phylogenetic ANCOVAs describe the same results between carnivorous and herbivorous species except for the pars rictalis and the *pars stegalis* (Table 2).

#### JAW MECHANICAL ADVANTAGES

The AMA of the pars rictalis ranges from  $0.32 \pm 0.07$  to  $0.63 \pm 0.06$  (mean  $\pm$  SD), of the *pars malaris* ranges from  $0.49 \pm 0.03$  to  $0.54 \pm 0.03$  and of the *pars stegalis* ranges from  $0.35 \pm 0.03$  to  $0.58 \pm 0.04$  in carnivorous and herbivorous species, respectively (Fig. 5A). The mean AMA of each muscle subdivision of the adductor mandibulae muscle is significantly greater

in herbivorous than in carnivorous species (Table 3), indicating that the adductor mandibulae muscle and its subdivisions transmit relatively more force to the front of the lower jaw in herbivorous species.

By contrast, the PMA of the pars rictalis ranges from  $0.87 \pm 0.06$  to  $0.92 \pm 0.09$ , of the *pars malaris* ranges from  $0.74 \pm 0.08$  to  $1.47 \pm 0.32$  and of the *pars stegalis* ranges from  $0.79 \pm 0.06$  to  $0.97 \pm 0.21$  in herbivorous and carnivorous species, respectively (Fig. 5B). Mean PMA values of the *pars malaris* and *pars stegalis* are significantly greater in carnivorous than in herbivorous species (Table 3), suggesting that the adductor mandibulae muscle and mainly both *pars malaris* and *pars stegalis* subdivisions transmit relatively more force to the back of the lower jaw in carnivorous species relative to herbivorous species. The AMA and PMA of the lepidophagous *Catoprion mento* are close to those of carnivorous species except for the *pars malaris*, which transmits relatively little force to the lower jaw.

#### TYPE OF JAW OCCLUSION

The quadrate offset distance in carnivorous species ranges from 0.09 in *Serrasalmus elongatus* to 0.41 in *Pygopristis denticulata* (Fig. 6). In herbivorous species, the quadrate offset distance ranges from 0.37 in *Acnodon oligacanthus* to 0.63 in *Myloplus rhomboidalis*. The specialist lepidophagous *Catoprion mento* has a quadrate offset distance of 0.30. Herbivorous species have a significantly higher mean quadrate offset distance ( $0.56 \pm 0.08$ ,

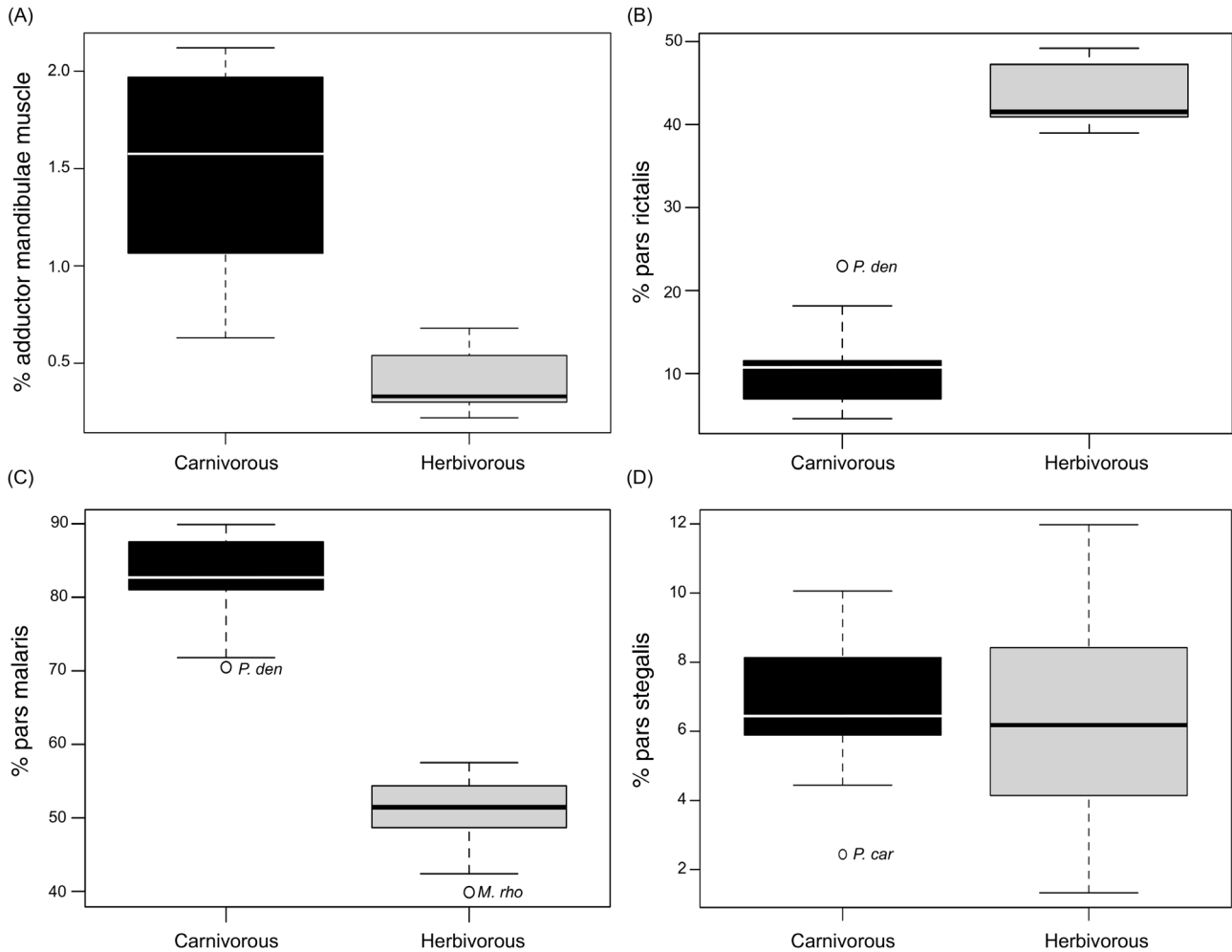


**Figure 4.** Boxplots of: (A) percentage of the adductor mandibulae muscle mass relative to body mass; (B) percentage of the pars rictalis mass; (C) percentage of the *pars malaris* mass; and (D) percentage of the pars stegalis mass relative to the total adductor mandibulae muscle mass in carnivorous and herbivorous species. Abbreviations of species names are given in [Table S1](#).

mean  $\pm$  SD) than carnivorous species ( $0.26 \pm 0.11$ ; [Table 3](#)). The distance between the quadrate–anguloarticular joint of the lower jaw and the dentition is therefore significantly greater in herbivorous species and their jaw occlusion resembles a ‘vice-like’ bite ([Fig. 6](#)). Conversely, this distance is lower in carnivorous species and their jaw occlusion resembles a ‘scissor-like’ bite.

#### LOWER JAW SHAPE

The centroid size of the lower jaw does not differ between carnivorous and herbivorous species (Procrustes ANOVA:  $F_{1,19} = 1.79$ ,  $P = 0.20$ ) but the two dietary groups show significant variation in lower jaw shape (Procrustes ANOVA:  $F_{1,19} = 56.79$ ,  $P = 0.001$ ; phylogenetic Procrustes ANOVA:  $F_{1,16} = 6.32$ ,  $P = 0.001$ ). The first three principal components (PC1 = 85%, PC2 = 7% and PC3 = 3%) account for 95% of the total

shape variation in the lower jaw. Along PC1 in the phylomorphospace ([Fig. 7](#)), positive scores are associated with herbivorous species such as the pacu *Piaractus brachypomus* for which lower jaws have an anteriorly contracted tooth row, a low dentary, a high coronoid process and a large anguloarticular bone. Negative scores are associated with carnivorous species such as the piranhas *Pygocentrus nattereri* or *Serrasalmus manuei* for which lower jaws have an expanded tooth row, an elongated dentary, a low coronoid process and a reduced anguloarticular bone. The piranha *Pygopristis denticulata* has an intermediate lower jaw shape between the species with negative and positive PC1 scores. Shape variation along PC2 ([Fig. 7](#)) is related to the height of the lower jaw. Positive scores are associated with shallow lower jaws whereas negative scores are associated with tall lower jaws. Both herbivorous and carnivorous species show variation in lower jaw height.

**Table 3.** Results of Mann–Whitney *U* tests and ANCOVAs for the functional morphological traits of the oral jaw system

	Mann–Whitney <i>U</i> tests		ANCOVAs				
	<i>U</i>	<i>P</i>	<i>df</i>	SS	MS	<i>F</i>	<i>P</i>
<b>Jaw muscle size</b>							
Adductor mandibulae muscle	106	<b>&lt;0.001</b>	18	0.56	0.03	26.23	<b>&lt;0.001</b>
Pars rictalis subdivision	0	<b>&lt;0.001</b>	18	0.39	0.02	14.33	<b>&lt;0.001</b>
<i>Pars malaris</i> subdivision	108	<b>&lt;0.001</b>	18	0.03	0.002	1072	<b>&lt;0.001</b>
Pars stegalis subdivision	60	0.7	18	0.89	0.05	23.08	<b>&lt;0.001</b>
<b>Jaw mechanical advantage</b>							
AMA pars rictalis	108	<b>&lt;0.001</b>					
AMA <i>pars malaris</i>	95	<b>&lt;0.01</b>					
AMA pars stegalis	108	<b>&lt;0.001</b>					
PMA pars rictalis	71.5	0.23					
PMA <i>pars malaris</i>	108	<b>&lt;0.001</b>					
PMA pars stegalis	81.5	<b>0.05</b>					
<b>Type of jaw occlusion</b>							
Quadrate offset distance	108	<b>&lt;0.001</b>					

Abbreviations: AMA, anterior mechanical advantage; PMA, posterior mechanical advantage; *df*, degrees of freedom; *F*, value of the *F*-statistic; MS, mean sum of squares; *P*, probability of significant difference between groups; SS, sum of squares; *U*, value of the non-parametric *U*-statistic. Significant values are given in bold type.

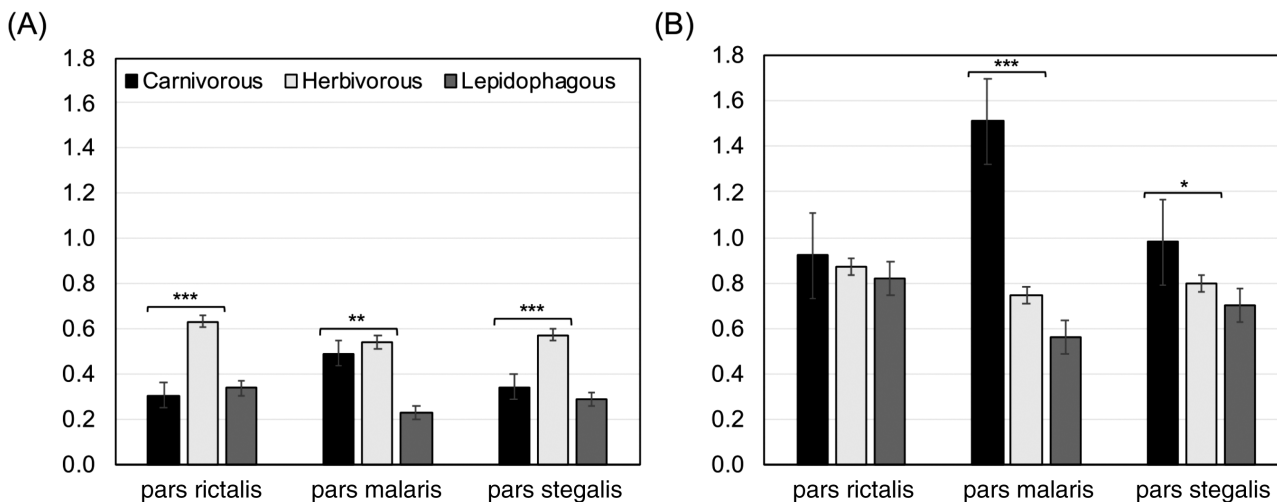


**Figure 5.** Bar graphs of anterior (A) and posterior (B) jaw mechanical advantages for the three subdivisions of the adductor mandibulae muscle (*pars rictalis*, *pars malaris* and *pars stegalis*) in serrasalmid species with different diet. *Catoprion mento* was not included in comparative statistical analyses. Error bars are the standard deviations and bars marked with an asterisk are significantly different (\* $P \leq 0.05$ ; \*\* $P \leq 0.01$ ; \*\*\* $P \leq 0.001$ ).

#### BITE FORCE AND FUNCTIONAL MORPHOLOGICAL TRAITS OF THE ORAL JAW SYSTEM

The adductor mandibulae muscle mass and the PMA of the *pars malaris* are the only functional morphological traits of the oral jaw system showing a linear relationship with  $BF_{in\ vivo}$ . In addition, these traits together provide the best multiple linear

model explaining the variability in  $BF_{in\ vivo}$  (stepwise multiple linear regression, final model:  $R^2 = 0.68$ ,  $P < 0.001$ ). However, using phylogenetically corrected methods, these results are no longer significant [phylogenetic linear regression  $BF_{in\ vivo} \sim$  adductor mandibulae muscle mass: Akaike information criterion (AIC) = 10.11,  $P = 0.89$ ; phylogenetic linear

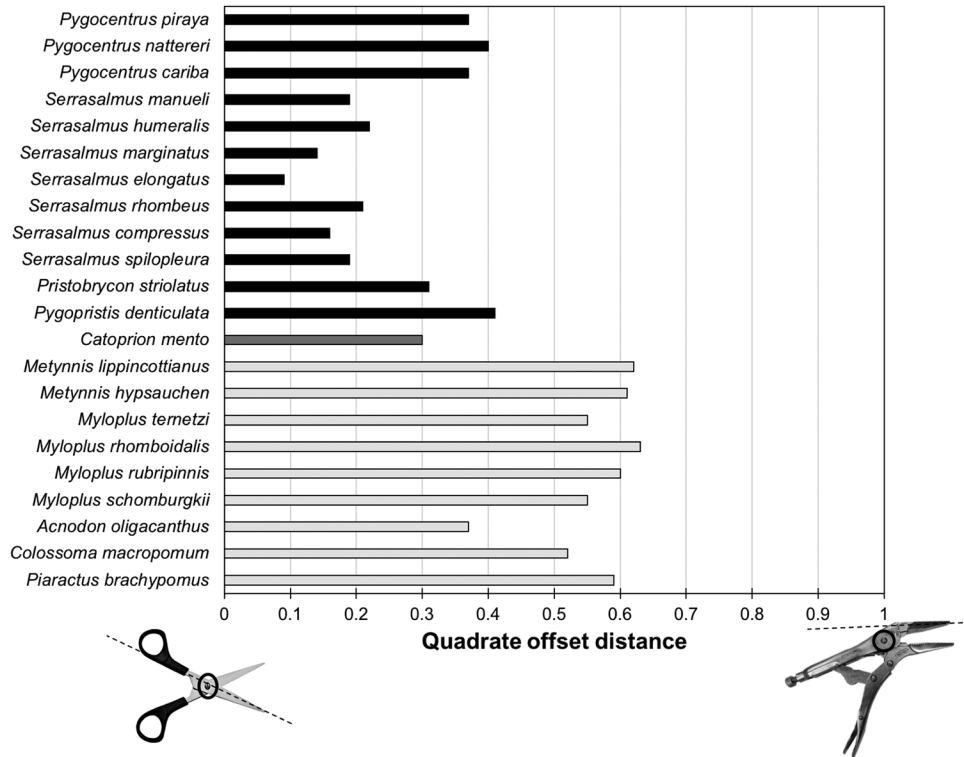


**Figure 6.** Bar graph of the mean quadrate offset distance in 22 serrasalmid species with different diet. Carnivorous species are represented by black bars, herbivorous species by light grey bars and the lepidophagous species *Catoprion mento* by a dark grey bar. A quadrate offset distance close to '0' represents a non-uniform jaw occlusion which corresponds to a perfect alignment between the jaw joint and the tooth row, while a quadrate offset distance close to '1' represents a uniform jaw occlusion which corresponds to an imperfect alignment between the jaw joint and the tooth row (Anderson, 2009).

regression  $BF_{in\ vivo} \sim PMA\ pars\ malaris$ : AIC = 9.29,  $P = 0.68$ ; phylogenetic stepwise multiple regression, initial model: AIC = 12.43,  $P > 0.05$ ).

## DISCUSSION

The present comparative study demonstrates that bite performance varies considerably within the highly specialized group of serrasalmid biters and that these variations may be related to diet. In addition, this study illustrates that morphological and functional traits of the oral jaw system vary in accordance with bite performance, diet specialization and evolutionary history within this Neotropical fish family.

### BITE PERFORMANCE AND DIET

In contrast to our predictions, herbivorous species that mainly feed by crushing hard plant items (fruits and seeds) do not have higher bite forces than carnivorous species that feed on soft animal prey (meat and flesh). Most studies linking diet to bite performance, however, have demonstrated that species with a more

durophagous diet have higher bite forces (Huber *et al.*, 2005; Mehta, 2008; Herrel & Holanova, 2008; Herrel *et al.*, 2017). Independent of the variation in body size, our data show that *in vivo* and theoretical bite forces are significantly higher in carnivorous than in herbivorous species, irrespective of the kind of 'herbivory' (Fig. 2A, B). This observation suggests that diet is probably the major driving force explaining this variation in bite performance. However, our results with phylogenetic correction provided only partial support for this hypothesis (Table 2). Consequently, we cannot reject the hypothesis that other factors may explain the observed divergence among trophic groups. Alternatively, the strong clustering of diet with clades may simply prevent us from detecting significant differences when taking phylogeny into account.

Furthermore, this observation also supports the suggestion that the carnivorous diet of piranhas requires powerful bite forces to capture and process prey (Grubich *et al.*, 2012), which are likely to be highly specific. The highest bite forces observed here were for *Pygocentrus nattereri* and *Pygocentrus piraya*, piranha species which usually attack in numbers live prey larger than themselves (Goulding, 1980; Jégu,

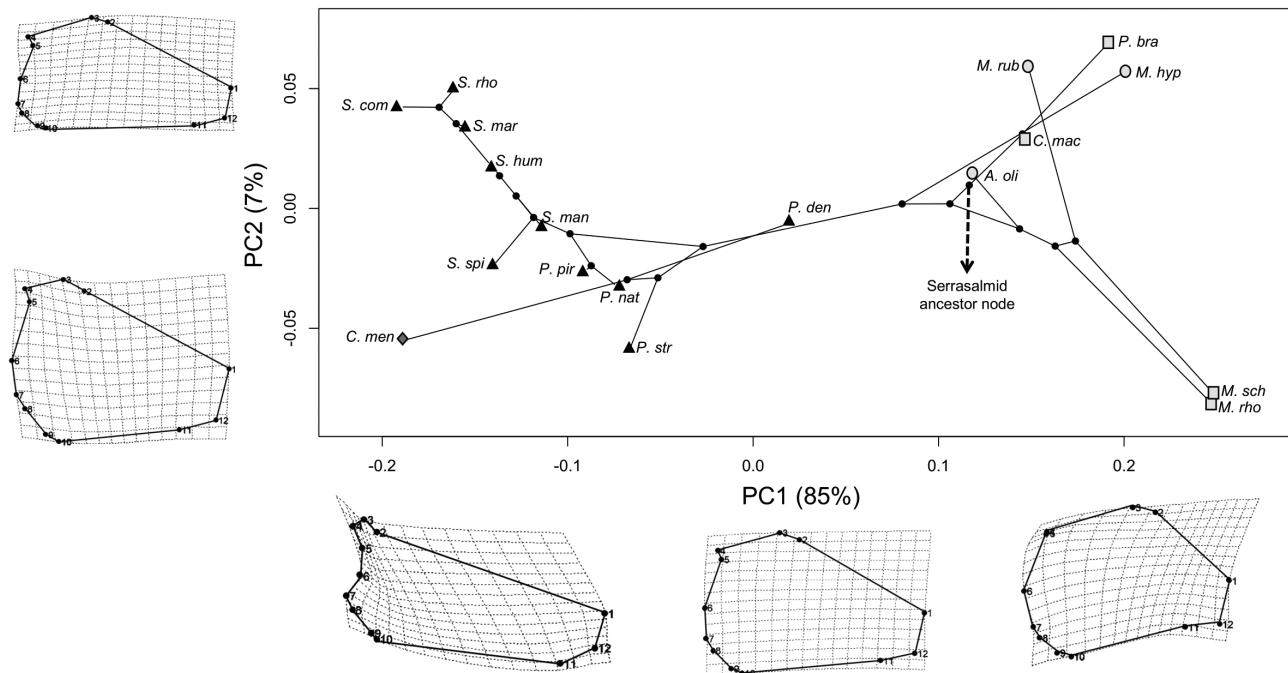


**Figure 7.** Phylomorphospace representing the shape variation of the right lower jaw along PC1 (85%) and PC2 (7%) axes in 18 serrasalmid species with different diet. Carnivorous species are represented by black triangles, herbivorous species feeding on hard plant items by light grey squares, herbivorous species feeding on soft plant items by light grey circles and the lepidophagous species *Catoprion mento* by a dark grey diamond. The horizontally and vertically aligned deformation grids help in the visualization of lower jaw shape variation along PC1 and PC2 axes, respectively. Abbreviations of species names are given in Table S1.

2003; Berkovitz, 2013). The size of the prey relative to consumer body size as well as the type of feeding behaviour might be the drivers of bite performance within carnivorous piranhas and herbivorous serrasalmid fishes. The piranha species with lower bite forces, *Serrasalmus compressus* and *Serrasalmus elongatus*, are reported to generally consume small prey items such as fins or scales of other fish (Goulding, 1980; Jégu, 2003). The specialized wimple-piranha *Catoprion mento* also eats mainly scales (Goulding, 1980; Jégu, 2003; Janovetz, 2005) and has the lowest bite force of any taxon in our study. This observation is consistent with previous studies on bite performance and prey size in other vertebrate groups. In lizards, higher bite forces are also associated with the consumption of large prey relative to body size (Herrel *et al.*, 2001; Verwajen *et al.*, 2002). Similar observations have been made for carnivorous mammals for which highest estimated bite forces were recorded in animals that usually kill and consume large prey (Wroe *et al.*, 2005; Christiansen & Wroe, 2007).

In herbivorous species, the issue of prey size might be compensated for by an increase in overall body size to improve bite performance, as suggested by Habegger *et al.* (2012) for bull sharks. The pacu species, *Colossoma macropomum*, *Piaractus mesopotamicus* and *Piaractus*

*brachypomus*, are known to be among the largest fish of the Amazon basin (Goulding & Carvalho, 1982) and they consume large fruits and seeds (Correa *et al.*, 2007). Being larger, these herbivorous species would thus have access to larger vegetal prey (e.g. Brazil nuts) than smaller herbivorous species such as *Metynnis hypsauchen*, *Metynnis lippincottianus*, *Myloplus rubripinnis* or *Myloplus ternetzi*. In addition, the high variability in  $BF_{in\ vivo}$  among herbivorous species (Fig. 2A) suggests this guild might be separated into two clusters: species feeding on hard plant items (fruits and seeds) with higher  $BF_{in\ vivo}$  and species feeding on soft plant items (algae, aquatic plants and flowers) with lower  $BF_{in\ vivo}$ . However, more detailed analyses of stomach contents and the relationship between food hardness and bite force are needed to reach clearer conclusions.

#### BITE PERFORMANCE AND FUNCTIONAL MORPHOLOGICAL DIVERSITY

Variation in bite performance between carnivorous and herbivorous serrasalmid species is supported by differences in the anatomy of the oral jaw system. The adductor mandibulae muscle is proportionally larger (Fig. 4A) with more sites origin of on the skull and

suspensorium (Table S2) in carnivorous compared to herbivorous species. A similar pattern is observed in granivorous finches (Fringillidae and Estrilidae) where fringillids can produce higher bite forces than estrildids of the same body size because they have relatively larger jaw closing muscles than estrildids (van der Meij & Bout, 2004). In air-breathing catfishes, an increase in bite force is also associated with hypertrophied jaw adductor muscles (Herrel *et al.*, 2002). The size of the adductor mandibulae muscle and the insertion site onto the lower jaw (Fig. 3C, D) are the main morphological traits of the oral jaw system that best predict bite force in serrasalmids. The largest adductor mandibulae muscle combined with the most anterior insertion of this muscle on the lower jaw provide the strongest bite force.

The morphological differences between carnivorous and herbivorous serrasalmid species also suggest different biomechanical functions and thus divergent bite strategies. Regarding the jaw muscle arrangement, the *pars rictalis* and *pars malaris* are the largest subdivisions of the adductor mandibulae muscle. They contribute more significantly to force transmission to the lower jaw than the *pars stegalis* and show more variation between dietary groups. The *pars rictalis* is larger in herbivorous (~40% of the total jaw muscle mass) than in carnivorous species (~10%), and, the *pars malaris* is more massive in carnivorous (~80%) than in herbivorous species (~50%). Moreover, these subdivisions have relatively ventral and dorsal origin sites on the suspensorium, respectively (Table S2). Force transmission is considered to be maximal when the muscle subdivisions are perpendicular to the axis passing by their insertion on the lower jaw and the jaw joint during mouth closing (Barel, 1983; Turingan, 1994). From this biomechanical point of view, the relatively vertical position of the *pars malaris* with respect to the lower jaw implies a better position for firmly grasping prey during mouth closing. Conversely, the relatively horizontal disposition of the *pars rictalis* suggests a better fit for speed. Carnivorous species might thus be more adapted to deliver powerful bite forces while firmly holding prey in the mouth. Herbivorous species might, by contrast be capable of generating faster bite forces; however, it must be borne in mind that real differences between the two diets represent trade-offs among different constraints (Parmentier *et al.*, 2000). In parallel, differences in physiological traits of the adductor mandibulae muscle (e.g. deep red, slow oxidative vs. intermediate vs. fast twitch muscle fibres) might also be a factor driving differences in bite abilities between dietary groups.

Furthermore, the arrangement of the *pars rictalis* and *pars malaris* is consistent with the lower jaw shape. In herbivorous species, the anteriorly shortened tooth row in association with larger coronoid process and anguloarticular bone provide a wider anterior

attachment site for the jaw muscles and mainly the *pars rictalis* (Fig. 3D). This ‘herbivorous configuration’ improves the in-lever arms and therefore gives better anterior mechanical advantages to the jaw system (Fig. 5A) to transmit powerful bite forces mainly at the front. In carnivorous species, the dentary is longer and possesses a greater number of larger, laterally oriented teeth. The coronoid process is reduced and the anguloarticular bone provides a limited attachment site for all jaw muscles (Fig. 3C). This ‘carnivorous configuration’ improves the posterior mechanical advantages of the jaw muscles (Fig. 5B) to generate more powerful bite forces at the back. In serrasalmid fishes, the mechanical advantage of the various muscle subdivisions can thus differ by either shifts in muscle insertion ( $L_{in}$ ) or length change in the lower jaw ( $L_{out}$ ). Note, however, that because mechanical advantages are dimensionless, these ratios can still end up being the same despite different anatomies.

Additionally, lower jaw shape may also be closely related to the bite strategy and diet specialization because the quadrate offset distance of herbivorous species is closer to ‘1’ compared with carnivorous species (Fig. 6). Quadrate offset values approximating ‘1’ have been shown to correspond to a near-perfect jaw occlusion and a ‘vice-like’ bite strategy in which all teeth occlude simultaneously in arthrodiros (Anderson, 2009). By contrast, quadrate offset values approximating ‘0’ have been shown to correspond to an imperfect jaw occlusion and a ‘scissor-like’ bite strategy in which two sides of the dentition occlude progressively from posterior to anterior (Anderson, 2009). Our data support that distinctive bite strategies may be found within a highly specialized fish group of biters. The acquisition of food in herbivorous species is mainly done using a close-to-vice-like bite strategy to crush fruits and seeds or to shear pieces of plants. Feeding in carnivorous species is primarily done using a close-to-scissor-like bite strategy to cut or slice pieces of fleshy prey. In addition to tooth shape differences between dietary groups, a scissor-like bite provides greater bite stresses due to the progression of the bite point across the occlusive surface. Conversely, a vice-like bite increases the bite surface area and therefore reduces bite stresses. Variation in the type of jaw occlusion and bite strategy has also been highlighted in sharks that crush hard-shelled molluscs compared to piscivorous sharks (Ramsay & Wilga, 2007). These authors further proposed that the shorter distance between the jaw joint and the dentition (i.e. imperfect jaw occlusion) may serve to maximize mouth gape to perform larger bites, as should certainly be the case for carnivorous piranhas as well.

The major differences in the oral jaw system of carnivorous and herbivorous serrasalmid species may represent an interesting functional parallelism

with mammals. In mammals, jaw closing is achieved by both masseter and temporalis muscles (Herring & Scapino, 1973; Herring *et al.*, 2001). The masseter muscle attaches on the zygomatic arch and on the lateral side of the mandible. It is mainly used to crush food at low gape angles. The temporalis muscle originates on the temporal bone of the skull and attaches on the coronoid process of the mandible. It allows the lower jaw to close at high speed (Schwenk, 2000) and provides optimal bite force at high gape. All mammals possess both muscles but the masseter muscle is usually larger and stronger in herbivorous than in carnivorous mammals whereas the temporalis muscle is larger in carnivorous species (Turnbull, 1970; Schwenk, 2000). Interestingly, these differences in the proportion of muscles are also related to lower jaw shape. In herbivorous mammals, the angular process is more expanded for the insertion of the masseter muscle whereas the coronoid process is proportionally more developed in carnivorous mammals in relation to the development of the temporal muscle (Schwenk, 2000). However, the increase in size of the coronoid process in carnivorous mammals, an adaptation for generating bite force at large gape, is not observed in carnivorous serrasalmid fishes where the coronoid process is reduced. Differences in jaw occlusion related to lower jaw shape have been highlighted in mammals as well (Turnbull, 1970; Herring & Herring, 1974; Greaves, 1982; Herring, 1993). In herbivorous mammals, the entire tooth rows of the upper and lower jaw contact the food simultaneously. Conversely, in carnivorous mammals the jaw joint is positioned low on the skull, providing these animals with a 'scissor-like' bite strategy.

#### EVOLUTIONARY HISTORY AND INTERMEDIATE MORPHOLOGY

In Serrasalminae, carnivory has been hypothesized to be a derived condition from the herbivorous or omnivorous diet of the common ancestor to modern serrasalmids based on maximum-likelihood ancestral character reconstructions of diet (Correa *et al.*, 2007). Previous studies on serrasalmid fishes (e.g. Gosline, 1951) also hypothesized that the single row of sharp teeth in carnivorous piranhas was derived from the two rows of large incisiform-to-molariform teeth in herbivorous species. However, we do not have information about the tempo of functional morphological evolution linked to this evolutionary shift in diet. The most likely hypothesis is that of a gradual morphological evolution requiring intermediate morphs as indicated by the serrasalmid fossil record and the intermediate zig-zag pattern of dentition of the presumed bone-crushing *Megapiranha paranensis* (Gayet & Meunier,

1998; Dahdul, 2004; Cione *et al.*, 2009; Grubich *et al.*, 2012).

Similarly, the extant *Pygopristis denticulata* has a single row of dentition with pentacuspoid teeth and an intermediate oral morphology between carnivorous and herbivorous species, supporting such a hypothesis. First, the size of the adductor mandibulae muscle of *Pygopristis denticulata* relative to its body mass is close to that of herbivorous species (Fig. S3A). Its pars rictalis subdivision is also more developed than in the other carnivorous species (Fig. 4B). The sites of origin of its pars rictalis are on both horizontal and vertical arms of the preoperculum as in herbivorous species (Table S2). Its pars malaris subdivision, however, is more developed than in herbivorous species (Fig. 4C). Its lower jaw thus shows an intermediate shape between the two dietary groups with an elongated dentary similar to carnivorous species but a large coronoid process and anguloarticular bone similar to herbivorous species (Fig. 7). *Pygopristis denticulata* might thus be an extant intermediate morph between two specialized serrasalmid groups. However, the fact that this species could also have an omnivorous diet explaining its intermediate oral morphology cannot be discarded because precise information about its diet are unavailable.

Finally, the serrasalmid family has undoubtedly diversified into various feeding habits that are all dependent on biting (herbivory, granivory, frugivory, carnivory, piscivory, lepidophagy, etc.). The extinct species *Megapiranha paranensis* is even considered to have been capable of piercing and crushing bones (i.e. osteophagy) following the hypothetical reconstruction of the jaw system from *Serrasalmus rhombeus* and estimations of bite performance (Grubich *et al.*, 2012). Along with our results, it might be hypothesized that the ability to generate strong bite forces is a derived biomechanical trait in the 'piranhas-clade' that evolved in response to their specific diet constraints.

#### CONCLUSION

To the best of our knowledge, this study represents the first time that such a large diversity in bite force and functional morphology of oral jaw system has been demonstrated in a fish group relying on a unique 'biting' feeding mode. In addition to the variation in dentition, our results highlight that the diet specialization towards carnivory in serrasalmid fishes has been accompanied by important changes in the size of the adductor mandibulae muscle (mainly the pars rictalis and pars malaris subdivisions) and lower jaw shape with major functional effects on bite performance and bite strategy. The increase in size

of the *pars malaris* subdivision at the expense of a decrease in size of the *pars rictalis*, in combination with an elongation of oral jaws and a greater number of highly specialized teeth, probably helped to increase bite force in an ancestor to modern serrasalmids. Furthermore, the decrease in size of the anguloarticular bone of the lower jaw, which shortens the quadrate offset distance, probably led to changes in the type of jaw occlusion in carnivorous species to closely match a 'scissor-like' bite.

#### ACKNOWLEDGEMENTS

This study was funded by the Belgian National Fund for Scientific Research (F.R.S.-FNRS, Research Project no. 23625340). A. Huby received an ASP – F.R.S.-FNRS Fellowship. The authors would like to thank the Patrimoine Foundations of the University of Liège for their grant support of the field mission in French Guiana in June 2017, and the 'Fonds Léopold III pour l'Exploration et la Conversation de la Nature' and the F.R.S.-FNRS for their grant support of the fieldwork in Brazil in July 2018. The authors are also extremely grateful to : the three heads of the Belgian public aquariums who allowed access to their amazing specimens, i.e. Philippe Jouk and keepers (Aquarium of the Antwerp ZOO), Christophe Remy and keepers (Museum of Natural History and Vivarium, Tournai) and Pierre Paulus (aquatic store 'J. Paulus et Fils SPRL', Marcinelle). We also thank the team of HYDRECO Guyane for their help with fish capture during the field expedition in French Guiana and Thiago Carvalho (Fundação Zoo-Botânica, Belo Horizonte) for his help during the field trip in Brazil. We also thank the authorities from Rio Doce State Park, Retiro Baixo Hydropower Plant and Campi Branco (Amador Aguiar) I & II HPP. We also thank Dr Geoffrey Mélotte for his help with maintaining fishes in the aquarium. Finally, we thank reviewers Dr Justin Grubich and Dr Nicolai Konow for their helpful comments and suggestions that improved the manuscript.

#### REFERENCES

- Adams DC, Collyer ML, Kaliontzopoulou A, Sherratt E. 2017. *Geomorph: software for geometric morphometric analyses*. R package version 3.0.5. <https://cran.r-project.org/web/packages/geomorph/index.html>. Accessed 30 March 2019.
- Adams DC, Otárola-Castillo E. 2013. Geomorph: an R package for the collection and analysis of geometric morphometric shape data. *Methods in Ecology and Evolution* **4**: 393–399.
- Adams DC, Rohlf FJ, Slice DE. 2013. A field comes of age: geometric morphometrics in the 21st century. *Hystrix, the Italian Journal of Mammalogy* **24**: 7–14.
- Aguirre LF, Herrel A, van Damme R, Matthysen E. 2002. Ecomorphological analysis of trophic niche partitioning in a tropical savannah bat community. *Proceedings of the Royal Society B: Biological Sciences* **269**: 1271–1278.
- Aguirre LF, Herrel A, Van Damme R, Matthysen E. 2003. The implications of food hardness for diet in bats. *Functional Ecology* **17**: 201–212.
- Albertson RC, Koehler TD. 2006. Genetic and developmental basis of cichlid trophic diversity. *Heredity* **97**: 211–221.
- Anderson PSL. 2009. Biomechanics, functional patterns, and disparity in Late Devonian arthropods. *Paleobiology* **35**: 321–342.
- Anderson RA, McBrayer LD, Herrel A. 2008. Bite force in vertebrates: opportunities and caveats for use of a nonpareil whole-animal performance measure. *Biological Journal of the Linnean Society* **93**: 709–720.
- Astley HC, Abbott EM, Azizi E, Marsh RL, Roberts TJ. 2013. Chasing maximal performance: a cautionary tale from the celebrated jumping frogs of Calaveras County. *Journal of Experimental Biology* **216**: 3947–3953.
- Azevedo MA. 2010. Reproductive characteristics of characid fish species (Teleostei, Characiformes) and their relationship with body size and phylogeny. *Iheringia. Série Zoologia* **100**: 469–482.
- Barel CDN. 1983. Towards a constructional morphology of cichlid fishes (Teleostei, Perciformes). *Netherlands Journal of Zoology* **33**: 357–424.
- Barnett A, Bellwood DR, Hoey AS. 2006. Trophic ecomorphology of cardinalfish. *Marine Ecology Progress Series* **322**: 249–257.
- Berkovitz BKB. 2013. *Nothing but the tooth: a dental odyssey*. Amsterdam: Elsevier Science.
- Bookstein FL. 1991. *Morphometric tools for landmark data: geometry and biology*. Cambridge: Cambridge University Press.
- Calcagnotto D, Schaefer SA, DeSalle R. 2005. Relationships among characiform fishes inferred from analysis of nuclear and mitochondrial gene sequences. *Molecular Phylogenetics and Evolution* **36**: 135–153.
- Christiansen P, Wroe S. 2007. Bite forces and evolutionary adaptations to feeding ecology in Carnivores. *Ecology* **88**: 347–358.
- Cione AL, Dahdul WM, Lundberg JG, Machado-Allison A. 2009. *Megapiranha paranensis*, a new genus and species of Serrasalminae (Characiformes, Teleostei) from the upper Miocene of Argentina. *Journal of Vertebrate Paleontology* **29**: 350–358.
- Collyer ML, Sekora DJ, Adams DC. 2015. A method for analysis of phenotypic change for phenotypes described by high-dimensional data. *Heredity* **115**: 357–365.
- Cooper WJ, Wernle J, Mann K, Albertson RC. 2011. Functional and genetic integration in the skulls of Lake Malawi cichlids. *Evolutionary Biology* **38**: 316–334.
- Correa SB, Winemiller KO, López-Fernández H, Galetti M. 2007. Evolutionary perspectives on seed consumption and dispersal by fishes. *BioScience* **57**: 748–756.

- Da Silva JM, Carne L, Measey GJ, Herrel A, Tolley KA. 2016.** The relationship between cranial morphology, bite performance, diet and habitat in a radiation of dwarf chameleon (*Bradypodion*). *Biological Journal of the Linnean Society* **119**: 52–67.
- Dahdul WM. 2004.** Fossil serrasalmine fishes (Teleostei: Characiformes) from the Lower Miocene of north-western Venezuela. *Special Papers in Palaeontology* **71**: 23–28.
- Datovo A, Vari RP. 2013.** The jaw adductor muscle complex in teleostean fishes: evolution, homologies and revised nomenclature (Osteichthyes: Actinopterygii). *PLoS ONE* **8**: e60846.
- De Schepper N, Van Wassenbergh S, Adriaens D. 2008.** Morphology of the jaw system in trichiurids: trade-offs between mouth closing and biting performance. *Zoological Journal of the Linnean Society* **152**: 717–736.
- Deban SM, Richardson JC. 2017.** A peculiar mechanism of bite-force enhancement in lungless salamanders revealed by a new geometric method for modeling muscle moments. *Journal of Experimental Biology* **220**: 3588–3597.
- Dollion AY, Measey GJ, Cornette R, Carne L, Tolley KA, da Silva JM, Boistel R, Fabre AC, Herrel A. 2017.** Does diet drive the evolution of head shape and bite force in chameleons of the genus *Bradypodion*? *Functional Ecology* **31**: 671–684.
- Dufour CM, Losos JB, Herrel A. 2018.** Do differences in bite force and head morphology between a native and an introduced species of anole influence the outcome of species interactions? *Biological Journal of the Linnean Society* **125**: 576–585.
- Dumont ER, Herrel A. 2003.** The effects of gape angle and bite point on bite force in bats. *Journal of Experimental Biology* **206**: 2117–2123.
- Erickson GM, Lappin AK, Vliet KA. 2003.** The ontogeny of bite-force performance in American alligator (*Alligator mississippiensis*). *Journal of Zoology* **260**: 317–327.
- Felsenstein J. 1985.** Phylogenies and the comparative method. *The American Naturalist* **125**: 1–15.
- Ferrara TL, Clausen P, Huber DR, McHenry CR, Peddemors V, Wroe S. 2011.** Mechanics of biting in great white and sandtiger sharks. *Journal of Biomechanics* **44**: 430–435.
- Frédérich B, Adriaens D, Vandewalle P. 2008a.** Ontogenetic shape changes in Pomacentridae (Teleostei, Perciformes) and their relationships with feeding strategies: a geometric morphometric approach. *Biological Journal of the Linnean Society* **95**: 92–105.
- Frédérich B, Pilet A, Parmentier E, Vandewalle P. 2008b.** Comparative trophic morphology in eight species of damselfishes (Pomacentridae). *Journal of Morphology* **269**: 175–188.
- Gayet M, Meunier FJ. 1998.** Maastrichtian to early Late Paleocene freshwater Osteichthyes of Bolivia: additions and comments. In: *Phylogeny and classification of neotropical fishes*. Porto Alegre: EDIPUCRS, 85–110.
- Géry J. 1972.** *Poissons characoïdes des Guyanes: I. Généralités; II. Famille des Serrasalminidae*. Leiden: EJ Brill.
- Ginot S, Herrel A, Claude J, Hautier L. 2018.** Skull size and biomechanics are good estimators of *in vivo* bite force in murid rodents. *The Anatomical Record* **301**: 256–266.
- Gosline WA. 1951.** Notes on the characid fishes of the subfamily Serrasalminae. *Proceedings of the California Academy of Sciences* **27**: 17–64.
- Goulding M. 1980.** *The fishes and the forest: explorations in Amazonian natural history*. Berkeley: University of California Press.
- Goulding M, Carvalho ML. 1982.** Life history and management of the tambaqui (*Colossoma macropomum*, Characidae): an important Amazonian food fish. *Revista Brasileira de Zoologia* **1**: 107–133.
- Greaves WS. 1982.** A mechanical limitation on the position of the jaw muscles of mammals: the one-third rule. *Journal of Mammalogy* **63**: 261–266.
- Greaves WS. 2002.** *The mammalian jaw: a mechanical analysis*. Cambridge: Cambridge University Press.
- Grubich JR, Huskey S, Crofts S, Orti G, Porto J. 2012.** Mega-Bites: extreme jaw forces of living and extinct piranhas (Serrasalminidae). *Scientific Reports* **2**: 1009.
- Habegger ML, Huber DH, Lajeunesse MJ, Motta PJ. 2017.** Theoretical calculations of bite force in billfishes. *Journal of Zoology* **303**: 15–26.
- Habegger ML, Motta PJ, Huber DR, Dean MN. 2012.** Feeding biomechanics and theoretical calculations of bite force in bull sharks (*Carcharhinus leucas*) during ontogeny. *Zoology* **115**: 354–364.
- Hammer Ø, Harper DA, Ryan PD. 2001.** PAST: paleontological statistics software package for education and data analysis. *Palaeontologia Electronica* **4**: 9.
- Harmon LJ, Weir JT, Brock CD, Glor RE, Challenger W. 2007.** GEIGER: investigating evolutionary radiations. *Bioinformatics* **24**: 129–131.
- Hernandez LP, Motta PJ. 1997.** Trophic consequences of differential performance: ontogeny of oral jaw crushing performance in the sheepshead, *Archosargus probatocephalus* (Teleostei, Sparidae). *Journal of Zoology* **243**: 737–756.
- Hernandez LP, Staab KL. 2015.** Bottom feeding and beyond: how the premaxillary protrusion of cypriniforms allowed for a novel kind of suction feeding. *Integrative and Comparative Biology* **55**: 74–84.
- Herrel A, Adriaens D, Verraes W, Aerts P. 2002.** Bite performance in clariid fishes with hypertrophied jaw adductors as deduced by bite modeling. *Journal of Morphology* **253**: 196–205.
- Herrel A, Castilla AM, Al-Sulaiti MK, Wessels JJ. 2014.** Does large body size relax constraints on bite-force generation in lizards of the genus *Uromastix*? *Journal of Zoology* **292**: 170–174.
- Herrel A, De Grauw E, Lemos-Espinal JA. 2001.** Head shape and bite performance in xenosaurid lizards. *Journal of Experimental Zoology* **290**: 101–107.
- Herrel A, Holanova V. 2008.** Cranial morphology and bite force in *Chamaeleolis* lizards – adaptations to molluscivory? *Zoology* **111**: 467–475.

- Herrel A, O'Reilly JC, Richmond AM. 2002.** Evolution of bite performance in turtles. *Journal of Evolutionary Biology* **15**: 1083–1094.
- Herrel A, Petrochic S, Draud M. 2017.** Sexual dimorphism, bite force and diet in the diamondback terrapin. *Journal of Zoology* **304**: 217–224.
- Herrel A, Podos J, Huber SK, Hendry AP. 2005.** Bite performance and morphology in a population of Darwin's finches: implications for the evolution of beak shape. *Functional Ecology* **19**: 43–48.
- Herrel A, Spithoven L, Van Damme R, De Vree F. 1999.** Sexual dimorphism of head size in *Gallotia galloti*: testing the niche divergence hypothesis by functional analyses. *Functional Ecology* **13**: 289–297.
- Herrel A, Vanhooydonck B, Van Damme R. 2004.** Omnivory in lacertid lizards: adaptive evolution or constraint? *Journal of Evolutionary Biology* **17**: 974–984.
- Herrel A, Van Damme R, Vanhooydonck B, De Vree F. 2001.** The implications of bite performance for diet in two species of lacertid lizards. *Canadian Journal of Zoology* **79**: 662–670.
- Herring SW. 1993.** Functional morphology of mammalian mastication. *American Zoologist* **33**: 289–299.
- Herring SW, Herring SE. 1974.** The superficial masseter and gape in mammals. *The American Naturalist* **108**: 561–576.
- Herring SW, Rafferty KL, Liu ZJ, Marshall CD. 2001.** Jaw muscles and the skull in mammals: the biomechanics of mastication. *Comparative Biochemistry and Physiology Part A* **131**: 207–219.
- Herring SW, Scapino RP. 1973.** Physiology of feeding in miniature pigs. *Journal of Morphology* **141**: 427–460.
- Huber DR, Eason TG, Hueter RE, Motta PJ. 2005.** Analysis of the bite force and mechanical design of the feeding mechanism of the durophagous horn shark *Heterodontus francisci*. *Journal of Experimental Biology* **208**: 3553–3571.
- Huber DR, Weggelaar CL, Motta PJ. 2006.** Scaling of bite force in the blacktip shark *Carcharhinus limbatus*. *Zoology* **109**: 109–119.
- Janovetz J. 2005.** Functional morphology of feeding in the scale-eating specialist *Catoprion mento*. *Journal of Experimental Biology* **208**: 4757–68.
- Jégu M. 2003.** Subfamily Serrasalminae (pacu and piranhas). In: Reis RE, Kullander SO, Ferraris CJ, eds. *Check list of the freshwater fishes of South and Central America*. Porto Alegre: EDIPUCRS, 182–196.
- Konow N, Bellwood DR. 2005.** Prey-capture in *Pomacanthus semicirculatus* (Teleostei, Pomacanthidae): functional implications of intramandibular joints in marine angelfishes. *Journal of Experimental Biology* **208**: 1421–1433.
- Konow N, Bellwood DR. 2011.** Evolution of high trophic diversity based on limited functional disparity in the feeding apparatus of marine angelfishes (f. Pomacanthidae). *PLoS ONE* **6**: e24113.
- Konow N, Price S, Abom R, Bellwood D, Wainwright P. 2017.** Decoupled diversification dynamics of feeding morphology following a major functional innovation in marine butterflyfishes. *Proceedings of the Royal Society B* **284**: 20170906.
- Lappin AK, Hamilton PS, Sullivan BK. 2006.** Bite-force performance and head shape in a sexually dimorphic crevice-dwelling lizard, the common chuckwalla [*Sauromalus ater* (= *obesus*)]. *Biological Journal of the Linnean Society* **88**: 215–222.
- Lappin AK, Wilcox SC, Moriarty DJ, Stoepller SAR, Evans SE, Jones MEH. 2017.** Bite force in the horned frog (*Ceratophrys cranwelli*) with implications for extinct giant frogs. *Scientific Reports* **7**: 11963.
- Liem KF. 1993.** Ecomorphology of the teleostean skull. In: Kanken J, Hall BK, eds. *The skull, Volume 3: functional and evolutionary mechanisms*. Chicago: University of Chicago Press, 422–452.
- Loeb GE, Gans C. 1986.** *Electromyography for experimentalists*. Chicago: University of Chicago Press.
- Mehta RS. 2008.** Ecomorphology of the moray bite: relationship between dietary extremes and morphological diversity. *Physiological and Biochemical Zoology* **82**: 90–103.
- van der Meij MAA, Bout RG. 2004.** Scaling of jaw muscle size and maximal bite force in finches. *The Journal of Experimental Biology* **207**: 2745–2753.
- van der Meij MAA, Bout RG. 2006.** Seed husking time and maximal bite force in finches. *Journal of Experimental Biology* **209**: 3329–3335.
- Mélotte G, Parmentier E, Michel C, Herrel A, Boyle K. 2018.** Hearing capacities and morphology of the auditory system in Serrasalminae (Teleostei: Otophysi). *Scientific Reports* **8**: 1281.
- Mélotte G, Vigouroux R, Michel C, Parmentier E. 2016.** Interspecific variation of warning calls in piranhas: a comparative analysis. *Scientific Reports* **6**: 36127.
- Meyers JJ, Nishikawa KC, Herrel A. 2018.** The evolution of bite force in horned lizards: the influence of dietary specialization. *Journal of Anatomy* **232**: 214–226.
- Moran CJ, Ferry L. 2014.** Bite force and feeding kinematics in the eastern North Pacific kyphosidae. *Journal of Experimental Zoology Part A: Ecological Genetics and Physiology* **321**: 189–197.
- Nico LG, Taphorn DC. 1988.** Food habits of piranhas in the low llanos of Venezuela. *Biotropica* **20**: 311–321.
- Nogueira MR, Peracchi AL, Monteiro LR. 2009.** Morphological correlates of bite force and diet in the skull and mandible of phyllostomid bats. *Functional Ecology* **23**: 715–723.
- Ortí G, Petry P, Porto JI, Jégu M, Meyer A. 1996.** Patterns of nucleotide change in mitochondrial ribosomal RNA genes and the phylogeny of piranhas. *Journal of Molecular Evolution* **42**: 169–182.
- Ortí G, Sivasundar A, Dietz K, Jégu M. 2008.** Phylogeny of the Serrasalminae (Characiformes) based on mitochondrial DNA sequences. *Genetics and Molecular Biology* **31**: 343–351.
- Parmentier E, Castro-Aguirre JL, Vandewalle P. 2000.** Morphological comparison of the buccal apparatus in two bivalve commensal Teleostei, *Encheliophis dubius* and *Onuxodon fowleri* (Ophidiiformes, Carapidae). *Zoomorphology* **120**: 29–37.
- Pelster B, Wood CM, Speers-Roesch B, Driedzic WR, Almeida-Val V, Val A. 2015.** Gut transport characteristics

- in herbivorous and carnivorous serrasalmid fish from ion-poor Rio Negro water. *Journal of Comparative Physiology B* **185**: 225–241.
- Pfaller JB, Herrera ND, Gignac PM, Erickson GM. 2010.** Ontogenetic scaling of cranial morphology and bite-force generation in the loggerhead musk turtle. *Journal of Zoology* **280**: 280–289.
- Powell PL, Roy RR, Kanim P, Bello MA, Edgerton VR. 1984.** Predictability of skeletal muscle tension from architectural determinations in guinea pig hindlimbs. *Journal of Applied Physiology* **57**: 1715–1721.
- Raadsheer MC, Van Eijden TMGJ, Van Ginkel FC, Prahl-Andersen B. 1999.** Contribution of jaw muscle size and craniofacial morphology to human bite force magnitude. *Journal of Dental Research* **78**: 31–42.
- Ramsay JB, Wilga CD. 2007.** Morphology and mechanics of the teeth and jaws of white-spotted bamboo sharks (*Chiloscyllium plagiosum*). *Journal of Morphology* **268**: 664–682.
- Rao X, Yang C, Ma L, Zhang J, Liang W, Møller AP. 2018.** Comparison of head size and bite force in two sister species of parrotbills. *Avian Research* **9**: 11.
- R Core Team. 2017.** R: A language and environment for statistical computing. <https://www.R-project.org/>. Accessed 30 March 2019.
- Revell LJ. 2009.** Size-correction and principal components for interspecific comparative studies. *Evolution: International Journal of Organic Evolution* **63**: 3258–3268.
- Revell LJ. 2012.** phytools: an R package for phylogenetic comparative biology (and other things). *Methods in Ecology and Evolution* **3**: 217–223.
- Rice KW, Buchholz R, Parsons GR. 2016.** Correlates of bite force in the Atlantic sharpnose shark, *Rhizoprionodon terraenovae*. *Marine Biology* **163**: 38.
- Rohlf FJ, Slice D. 1990.** Extensions of the Procrustes method for the optimal superimposition of landmarks. *Systematic Zoology* **39**: 40–59.
- Santana SE, Dumont ER, Davis JL. 2010.** Mechanics of bite force production and its relationship to diet in bats. *Functional Ecology* **24**: 776–784.
- Schwenk K. 2000.** *Feeding form, function, and evolution in tetrapod vertebrates*. Amsterdam: Elsevier.
- Shellis RP, Berkovitz BKB. 1976.** Observations on the dental anatomy of piranhas (Characidae) with special reference to tooth structure. *Journal of Zoology* **180**: 69–84.
- Thomas P, Pouydebat E, Hardy I, Aujard F, Ross CF, Herrel A. 2015.** Sexual dimorphism in bite force in the grey mouse lemur. *Journal of Zoology* **296**: 133–138.
- Thompson AW, Betancur RR, López-Fernández H, Ortí G. 2014.** A time-calibrated, multi-locus phylogeny of piranhas and pacus (Characiformes: Serrasalminae) and a comparison of species tree methods. *Molecular Phylogenetics and Evolution* **81**: 242–257.
- Turingan RG. 1994.** Ecomorphological relationships among Caribbean tetraodontiform fishes. *Journal of Zoology* **233**: 493–521.
- Turnbull WD. 1970.** Mammalian masticatory apparatus. *Journal of Mammalogy* **52**: 482–484.
- Verwajen D, Van Damme R, Herrel A. 2002.** Relationships between head size, bite force, prey handling efficiency and diet in two sympatric lacertid lizards. *Functional Ecology* **16**: 842–850.
- Wainwright PC. 1988.** Morphology and ecology: functional basis of feeding constraints in Caribbean labrid fishes. *Ecology* **69**: 635–645.
- Wainwright PC, Bellwood DR, Westneat MW, Grubich JR, Hoey AS. 2004.** A functional morphospace for the skull of labrid fishes: patterns of diversity in a complex biomechanical system. *Biological Journal of the Linnean Society* **82**: 1–25.
- Van Wassenbergh S, Herrel A, James RS, Aerts P. 2007.** Scaling of contractile properties of catfish feeding muscles. *Journal of Experimental Biology* **210**: 1183–1193.
- Westneat MW. 2003.** A biomechanical model for analysis of muscle force, power output and lower jaw motion in fishes. *Journal of Theoretical Biology* **223**: 269–281.
- Westneat MW. 2004.** Evolution of levers and linkages in the feeding mechanisms of fishes. *Integrative and Comparative Biology* **44**: 378–389.
- Wroe S, Huber DR, Lowry M, McHenry C, Moreno K, Clausen P, Ferrara TL, Cunningham E, Dean MN, Summers AP. 2008.** Three-dimensional computer analysis of white shark jaw mechanics: how hard can a great white bite? *Journal of Zoology* **276**: 336–342.
- Wroe S, McHenry C, Thomason J. 2005.** Bite club: comparative bite force in big biting mammals and the prediction of predatory behaviour in fossil taxa. *Proceedings of the Royal Society B: Biological Sciences* **272**: 619–625.

## SUPPORTING INFORMATION

Additional Supporting Information may be found in the online version of this article at the publisher's web-site.

**Figure S1.** Phylogenetic relationships and diet in 40 serrasalmid species based on molecular data from [Thompson \*et al.\* \(2014\)](#). The original tree was pruned to include only species examined in our study (in black) and to exclude species that were not studied (in grey). Nine additional species investigated here (*Metynniss lippincottianus*, *Metynniss maculatus*, *Myleus micans*, *Myloplus ternetzi*, *Piaractus mesopotamicus*, *Pygocentrus cariba*, *Serrasalmus brandtii*, *Serrasalmus elongatus* and *Serrasalmus maculatus*) were not studied in the original phylogeny and were thus not included in the phylogenetic comparative analyses. The diet of carnivorous species is represented by a red dot, that of herbivorous species by a green dot and that of the lepidophagous species *Catoprion mento* by a black dot.

**Figure S2.** Photographs of the dentition in (A) the carnivorous *Pygocentrus nattereri* and (B) the herbivorous *Piaractus brachipomus*.

**Figure S3.** Linear regressions of (A)  $\log_{10}$ -transformed adductor mandibulae muscle mass against  $\log_{10}$ -transformed body mass ( $\log_{10}$  BM) and (B)  $\log_{10}$ -transformed pars rictalis mass, (C)  $\log_{10}$ -transformed *pars malaris* mass and (D)  $\log_{10}$ -transformed pars stegalis mass against  $\log_{10}$ -transformed adductor mandibulae muscle mass in 22 serrasalmid species with different diet. Key in A applies also to B–D. *Catoprion mento* was not included in comparative statistical analyses. In A, regression line equations are  $\log_{10}$  adductor mandibulae muscle mass =  $0.95 \log_{10} \text{ BM} - 1.77$  ( $R^2 = 0.87$ ) for carnivorous species and  $\log_{10}$  adductor mandibulae muscle mass =  $0.84 \log_{10} \text{ BM} - 2.77$  ( $R^2 = 0.61$ ) for herbivorous species. In B, these equations are  $\log_{10}$  pars rictalis mass =  $1.22 \log_{10}$  adductor mandibulae muscle mass -  $0.9$  ( $R^2 = 0.91$ ) for carnivorous species and  $\log_{10}$  pars rictalis mass =  $1.0 \log_{10}$  adductor mandibulae muscle mass -  $0.36$  ( $R^2 = 0.98$ ) for herbivorous species. In C, these equations are  $\log_{10}$  *pars malaris* mass =  $0.98 \log_{10}$  adductor mandibulae muscle mass -  $0.1$  ( $R^2 = 0.99$ ) for carnivorous species and  $\log_{10}$  *pars malaris* mass =  $0.95 \log_{10}$  adductor mandibulae muscle mass -  $0.34$  ( $R^2 = 0.97$ ) for herbivorous species. In D, these equations are  $\log_{10}$  pars stegalis mass =  $1.1 \log_{10}$  adductor mandibulae muscle mass -  $1.15$  ( $R^2 = 0.91$ ) for carnivorous species and  $\log_{10}$  pars stegalis mass =  $1.4 \log_{10}$  adductor mandibulae muscle mass -  $0.91$  ( $R^2 = 0.69$ ) for herbivorous species. Abbreviations of species names are given in Table S1.

**Table S1.** List of the abbreviations of species names used in this comparative study and additional references on serrasalmid diet.

**Table S2.** Summary of the sites of origin of the three subdivisions of the adductor mandibulae muscle (pars rictalis, *pars malaris* and pars stegalis) in 22 serrasalmid species with different diet.

**Text S1.** Additional information about sampling, provenance and maintenance of serrasalmid species.

**Text S2.** Calculation of theoretical bite forces.